Inter-robot Transformations in 3D

Nikolas Trawny, *Student Member, IEEE,* Xun S. Zhou, *Student Member, IEEE,* Ke Zhou, *Student Member, IEEE,* and Stergios I. Roumeliotis, *Member, IEEE*

***Abstract*—In this paper, we provide a study of motion-induced 3D extrinsic calibration based on robot-to-robot sensor measurements. In particular, we introduce algebraic methods to compute the relative translation and rotation between two robots using known robot motion and robot-to-robot (i) distance and bearing, (ii) bearing-only, and (iii) distance-only measurements. We further conduct a nonlinear observability analysis and provide sufficient conditions for the 3D relative position and orientation (pose) to become locally weakly observable. Finally, we present a nonlinear weighted least squares estimator to refine the algebraic pose estimate in the presence of noise. We use simulations to evaluate the performance of our methods in terms of accuracy and robustness.**

***Index Terms*—3D extrinsic calibration, cooperative localization.**

I. Introduction

In robotic applications such as localization [1]–[5], mapping [6]–[10], and tracking [11]–[15], the benefits of deploying cooperating teams instead of single robots have been widely recognized. A group of robots can combine measurements from many geographically dispersed locations and different vantage points, resulting in increased estimation accuracy. However, such sensor-fusion algorithms usually require that the measurements are expressed with respect to a common frame of reference. This in turn requires knowledge of the 6 degrees of freedom (d.o.f.) transformation between the robots, i.e., the robot-to-robot relative position and orientation (pose).

Most cooperative estimation algorithms operate under the assumption that the sensor-to-sensor transformation is externally provided. However, very few works describe how this transformation can be found. In general, the relative pose of two robots can be measured manually, inferred indirectly from individual localization with respect to a common frame of reference (e.g., using GPS), or determined by spatially correlating overlapping sensor measurements (e.g., visual feature matching). These methods are time-consuming, may not be sufficiently accurate, or may even be infeasible in adverse environments (e.g., in GPS-denied or textureless areas).

Alternatively, the relative pose can be computed using robot-to-robot relative observations, resulting from range sensors, bearing sensors, or both. In 2D, the relative pose can be determined in closed form from a single set of robot-to-robot distance and bearing measurements [1], [16]. In 3D, however, the robots will necessarily have to move and take multiple measurements from different vantage points in order to uniquely determine the interrobot transformation (see Section IV). This task of motion-induced 6 d.o.f. robot-to-robot extrinsic calibration is precisely the problem under investigation in this paper (see Fig. 1).

N. Trawny, X. S. Zhou, and S. I. Roumeliotis are with the Department of Computer Science and Engineering; K. Zhou is with the Department of Electrical and Computer Engineering, University of Minnesota, Minneapolis, MN, 55455 USA e-mail: {trawny|zhou|kezhou|stergios}@cs.umn.edu.

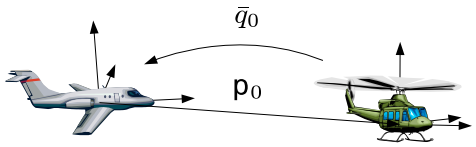

Fig. 1. This paper addresses the problem of determining the spatial configuration of mobile robots in 3D, i.e., their relative position $\mathbf{p}_0$ and orientation $\bar{q}_0$, based on robot-to-robot distance and/or bearing measurements. Note that measurements from several vantage points are required to uniquely determine the robots' relative transformation.

Estimating the relative pose of multiple robots can generally be cast as a nonlinear optimization problem [e.g., nonlinear Weighted Least Squares (WLS)], and solved by iterative methods, such as Gauss-Newton. The quality of the result, however, invariably depends on the accuracy of the *initial estimate* used to start the solver. If no initial estimate is available, the WLS algorithm can be initialized with a random guess, but may take an excessive number of iterations to converge, or may even diverge.

The main contributions of this paper are twofold: (i) We introduce algorithms that provide accurate, fast, closed-form estimates of the relative pose of two robots, which can be used stand-alone or to initialize an iterative refinement process. All methods are shown to be exact in the absence of measurement noise. In particular, we investigate analytical algorithms for the cases where the robots are equipped with 6 d.o.f. motion sensors, as well as robot-to-robot range sensors, bearing sensors, or both. (ii) We present a nonlinear observability study based on Lie derivatives and provide sufficient conditions for the robot-to-robot relative pose to become locally weakly observable. We have tested our algorithms extensively in simulation and evaluated their performance both stand-alone and as initial guess for WLS refinement. The presented results underline their clear superiority over a random WLS initialization in terms of speed of convergence and robustness. In our previous publications related to this work, we provided closed-form algorithms to determine the relative pose in 2D [17] and 3D [18], [19] from *range-only* robot-to-robot measurements. The present paper substantially extends this work by including algorithms for the cases of *3D bearing-only* and *range and bearing* sensors, as well as the *nonlinear observability study for all three cases*. The algorithm for the 3D range measurement case presented in Section VI is the linear algorithm to determine the unique solution using at least 10 distance measurements discussed in [18]. Alternatively, especially in the presence of outliers, one can use the method presented

in [19] to solve several minimal subproblems (40 solutions using 6 distance measurements), and obtain the unique solution using clustering. This approach is considerably more involved, and does not fit our premise of providing fast, closed-form estimates.

The remainder of this paper is organized as follows: After situating our work with respect to existing literature in Section II, we describe our algorithms for range and bearing, bearing-only, and range-only measurements in Sections IV, V, and VI, respectively. Section VII provides the observability analysis of these three cases. The WLS refinement is discussed in Section VIII, followed by the simulation results in Section IX, and concluding remarks in Section X.

II. Literature Review

Recent research on leveraging sensor-to-sensor measurements to solve the relative localization problem has focussed primarily on *static* sensor networks. These approaches only determine the *position* of sensor nodes, not their relative orientation. Static sensor networks cannot overcome this fundamental limitation, since at least one sensor (if not both) must move for the 3D pose to become observable (see Section VII). Localization algorithms for static sensor networks infer the node positions using measurements to so-called anchor nodes with known global position. The position of the remaining sensors in the network can be uniquely determined if certain graph-rigidity constraints are satisfied [20]. A number of algorithms for 2D node localization have been proposed based on convex optimization [21], multidimensional scaling [22], or graph connectivity [23]. In 3D, flying anchor nodes have been proposed to localize sensors, for example, an unmanned aerial vehicle aiding static sensor network localization [24], or a single satellite localizing a stationary planetary rover using distance measurements [25].

For many practical applications, such as tracking or sensor fusion, knowledge of both relative sensor position *and* orientation is required. Relative pose estimation in static 2D sensor networks, using a combination of distance and bearing measurements, was recently shown to be NP-hard [26]. For mobile robots, the problem of relative pose determination has only been thoroughly investigated in 2D. It is known that mutual distance and bearing measurements from a single vantage point are sufficient to determine the full relative pose in closed-form [1], [16]. However, when only distance or bearing measurements are available, the robots must move between observations. The relative pose can then be found by combining the estimated robot motion (e.g., from odometry) and the mutual bearing [27] or distance [17] measurements. The nonlinear observability study by Martinelli and Siegwart [27] provides sufficient conditions for the pose to become observable for all three cases of relative observations.

In 3D, however, there exists very little literature on determining the relative pose using sensor-to-sensor measurements. Our paper is intended to fill this gap. Notice that by careful instrumentation of the robots, it is possible to estimate relative pose from a single set of measurements without requiring motion of the robots. In these cases, the sensors can effectively acquire multiple distance and/or bearing measurements simultaneously, for example using distance measurements between arrays of rigidly connected sensors [28], or by using calibrated cameras measuring a specially designed calibration target on the other robot [29], [30]. Such simultaneous measurements greatly simplify the solution, but are only applicable in sufficiently close range, where the spatial extent of the target is well within the sensor resolution. Instead, this paper focuses on single, point-to-point distance and bearing measurements, which is also valid for long distance measurements.

To our knowledge, no algorithms exist for the specific task of relative pose estimation using robot-to-robot *distance and bearing* or *bearing-only* measurements. In this paper, we introduce two algorithms to solve these problems. Moreover, only few works address the more challenging case of computing relative pose from *distance-only* measurements. In the most general, minimal problem case, the task of relative pose estimation using only distance measurements is actually equivalent to the forward kinematics problem of the general Stewart-Gough mechanism [31]. This parallel manipulator consists of a base platform and a moving platform connected by six articulated legs of variable lengths. The forward kinematics problem is to determine the relative pose of the base and the end effector given the six leg lengths and the coordinates of the leg attachment points in the base and end effector frames, respectively. This problem has 40 (generally complex) solutions [32], which can be found based on nonlinear techniques from algebraic geometry [19], [33], [34]. In contrast, we introduce a linear method using 10 distance measurements to uniquely determine the relative pose of robots navigating in 3D [18]. In particular, our method uses lifting, i.e., the linearization of an overdetermined system of polynomials by introducing new variables.

In this paper, we seek to provide an overarching treatment of 3D pose determination based on sensor-to-sensor measurements. To this end, we present closed-form algorithms, as well as a nonlinear observability analysis for all three cases of robot-to-robot distance-only, bearing-only, or distance and bearing measurements. We start our discussion in the next section with the problem formulation and a brief review of basic quaternion algebra.

III. Problem Formulation

A. Notation

In order to improve the clarity of presentation, we hereafter introduce most of the notation used throughout the paper.

- $_i\mathbf{p}_j$ Position of frame $\{j\}$ expressed in frame $\{i\}$.
- $_j^i\mathbf{C}$ Rotational matrix that projects vectors expressed in frame $\{j\}$ to frame $\{i\}$.
- d_k The distance between two robots at time-step k.
- $\mathbf{b}_{1,k}$ Bearing from robot R_1 to R_2 at time-step k, expressed in R_1's local frame.
- $\mathbf{b}_{2,k}$ Bearing from robot R_2 to R_1 at time-step k, expressed in R_2's local frame.

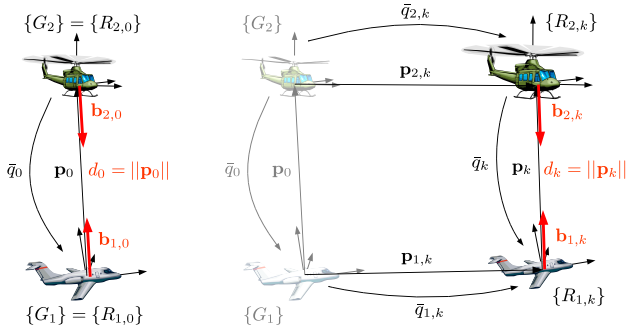

Fig. 2. Geometry of the robot trajectories. (a) Both robots meet for the first time ($k = 0$). Without loss of generality, we assume that at this point, local and global frames coincide. (b) At time k, both robots $i = \{1, 2\}$ have moved. We assume that both robots can estimate their pose $\bar{q}_{i,k}$, $\mathbf{p}_{i,k}$ in their own global frames, and measure distance d_k and/or bearing $\mathbf{b}_{i,k}$ to the other robot. The problem is to determine the transformation between the global frames, i.e., $\mathbf{p}_0$, and $\bar{q}_0$.

Consider two robots[1], R_1 and R_2, moving randomly in 3D space (see Fig. 2). At the point when the robots meet for the first time, let the frames of reference attached to the robots, $\{R_{1,0}\}$ and $\{R_{2,0}\}$, coincide with their global frames $\{G_1\}$ and $\{G_2\}$. Our objective is to determine the 6 d.o.f. transformation between these two global frames.

Further along their trajectories, the robots reach positions $\mathbf{p}_{1,k} := {}^{G_1}\mathbf{p}_{R_{1,k}}$ and $\mathbf{p}_{2,k} := {}^{G_2}\mathbf{p}_{R_{2,k}}$, $k = 1, \ldots, n-1$, which they can each estimate with respect to their own global frame (e.g., from integrating velocity measurements over time). We further denote the robots' current orientation using the rotation matrices $\mathbf{C}_{1,k} := {}^{R_{1,k}}_{G_1}\mathbf{C}$ and $\mathbf{C}_{2,k} := {}^{R_{2,k}}_{G_2}\mathbf{C}$, or the corresponding unit quaternions $\bar{q}_{1,k}$ and $\bar{q}_{2,k}$.

Let us also consider the vector $\mathbf{p}_k := {}^{R_{1,k}}\mathbf{p}_{R_{2,k}}$ from robot R_1 to robot R_2 at time k, and the relative orientation between the two robots' local frames, described by the rotation matrix $\mathbf{C}_k := {}^{R_{1,k}}_{R_{2,k}}\mathbf{C}$ or the corresponding quaternion $\bar{q}_k$. The 6 d.o.f. transformation between the global frames is parameterized by the translation ${}^{G_1}\mathbf{p}_{G_2}$ and rotation ${}^{G_1}_{G_2}\mathbf{C}$. Since we assumed that the robots started at their respective global frames, these unknown variables are equal to $\mathbf{p}_0$ and $\mathbf{C}_0$ (or $\bar{q}_0$).

At every time step $k = 0, \ldots, n-1$, each robot can record a measurement of the range and/or bearing towards the other robot, for a total of n pairs of robot-to-robot measurements. The distance between the robots is given by $d_k = ||\mathbf{p}_k||_2 = \sqrt{\mathbf{p}_k^T \mathbf{p}_k}$, and the bearing is described by either a unit vector in the current local frame, or the observation of a calibrated pinhole camera. Denoting the components of $\mathbf{p}_k$ as $\mathbf{p}_k = \begin{bmatrix} x & y & z \end{bmatrix}^T$, robot R_1 then observes the bearing $\mathbf{b}_{1,k} := \begin{bmatrix} \frac{x}{z} & \frac{y}{z} \end{bmatrix}^T$ to robot R_2, or the corresponding unit vector $\bar{\mathbf{b}}_{1,k} := \frac{\mathbf{p}_k}{||\mathbf{p}_k||}$. Similarly, robot R_2 can measure $\mathbf{b}_{2,k}$ or the corresponding unit vector $\bar{\mathbf{b}}_{2,k}$ in its current local frame. Later, we will also need these unit vectors rotated in the corresponding global frames for which we define the symbols ${}^{G_1}\bar{\mathbf{b}}_{1,k} := \mathbf{C}_{1,k}^T \bar{\mathbf{b}}_{1,k}$ and ${}^{G_2}\bar{\mathbf{b}}_{2,k} := \mathbf{C}_{2,k}^T \bar{\mathbf{b}}_{2,k}$.

[1]In this paper, we will present methods to find the relative pose between two robots. The extension to N robots is straightforward.

In what follows, we investigate three cases of finding the relative global transformation: (i) using both distance and bearing measurements, (ii) using only bearing measurements, and (iii) using only distance measurements. We introduce algebraic methods that yield a closed-form, non-iterative solution for the relative transformation. In the presence of noise, this solution is a sub-optimal estimate of the relative pose, but can serve as a precise initial guess for an iterative optimal estimation algorithm, such as the nonlinear WLS method described in Section VIII.

Before delving into the details of the algorithms for analytically computing the 3D robot-to-robot transformation, we first provide a brief overview of quaternion algebra, whose results and notation will be needed in the remainder of the paper.

B. Quaternion Algebra

We parameterize rotation using a 4×1 unit quaternion

$$\bar{q} = \begin{bmatrix} q_1 & q_2 & q_3 & q_4 \end{bmatrix}^T = \begin{bmatrix} \mathbf{q}^T & q_4 \end{bmatrix}^T, \qquad \bar{q}^T \bar{q} = 1 \quad (1)$$

Employing the (non-Hamiltonian) conventions for quaternions specified in [35], the rotation of frame $\{1\}$ with respect to frame $\{2\}$ can be expressed by the rotation matrix ${}^2_1\mathbf{C}({}^2_1\bar{q})$ whose entries are quadratic in the elements of ${}^2_1\bar{q}$

$$\mathbf{C}(\bar{q}) = (q_4^2 - \mathbf{q}^T\mathbf{q})\mathbf{I}_3 - 2q_4\lfloor \mathbf{q} \times \rfloor + 2\mathbf{q}\mathbf{q}^T \quad (2)$$

where $\mathbf{I}_3$ is the 3×3 identity matrix, and the symbol $\lfloor \mathbf{q} \times \rfloor$ denotes the skew-symmetric 3×3 matrix corresponding to the cross-product, so that

$$\mathbf{q} \times \mathbf{p} = \lfloor \mathbf{q} \times \rfloor \mathbf{p} = \begin{bmatrix} 0 & -q_3 & q_2 \\ q_3 & 0 & -q_1 \\ -q_2 & q_1 & 0 \end{bmatrix} \mathbf{p} \quad (3)$$

Using these conventions, the product of two rotation matrices equals the rotation matrix corresponding to the product of their associated quaternions, i.e.,

$$\mathbf{C}(\bar{p})\mathbf{C}(\bar{q}) = \mathbf{C}(\bar{p} \otimes \bar{q}) \quad (4)$$

The symbol "$\otimes$" in the above equation denotes quaternion multiplication, which can be written equivalently as a matrix multiplication:

$$\bar{p} \otimes \bar{q} = \mathcal{L}(\bar{p})\bar{q} = \mathcal{R}(\bar{q})\bar{p} \quad (5)$$

where

$$\mathcal{L}(\bar{p}) = \begin{bmatrix} \mathbf{\Psi}(\bar{p}) & \bar{p} \end{bmatrix}, \qquad \mathbf{\Psi}(\bar{p}) = \begin{bmatrix} p_4\mathbf{I}_3 - \lfloor \mathbf{p} \times \rfloor \\ -\mathbf{p}^T \end{bmatrix} \quad (6)$$

$$\mathcal{R}(\bar{q}) = \begin{bmatrix} \mathbf{\Xi}(\bar{q}) & \bar{q} \end{bmatrix}, \qquad \mathbf{\Xi}(\bar{q}) = \begin{bmatrix} q_4\mathbf{I}_3 + \lfloor \mathbf{q} \times \rfloor \\ -\mathbf{q}^T \end{bmatrix} \quad (7)$$

The identity and the inverse element with respect to multiplication are given by

$$\bar{q}_I = \begin{bmatrix} \mathbf{0}_{1\times 3} & 1 \end{bmatrix}^T, \qquad \bar{q}^{-1} = \begin{bmatrix} -\mathbf{q}^T & q_4 \end{bmatrix}^T \quad (8)$$

Using the unit quaternion parameterization, the rotation of a vector from frame $\{1\}$ to frame $\{2\}$ can be expressed as

$${}^2\mathbf{v} = {}^2_1\mathbf{C}({}^2_1\bar{q})\,{}^1\mathbf{v} \;\Leftrightarrow\; \begin{bmatrix} {}^2\mathbf{v} \\ 0 \end{bmatrix} = {}^2_1\bar{q} \otimes \begin{bmatrix} {}^1\mathbf{v} \\ 0 \end{bmatrix} \otimes {}^2_1\bar{q}^{-1} \quad (9)$$

More details about quaternion algebra can be found in [36].

IV. 3D Relative Pose from Range and Bearing Measurements

The first case for which we present an analytic solution to the 6 d.o.f. relative pose estimation problem is the one where the robots are equipped with both range *and* bearing sensors. We first compute the relative attitude using only the bearing (unit vector) measurements. In the next step, we use this attitude estimate and the relative distance measurements to compute the relative translation of the robots' global frames.

A. Relative Attitude

Each pair of unit vector measurements recorded by the two robots can be used in a constraint of the form

$$ {}^{G_1}\bar{\mathbf{b}}_{1,k} = -\mathbf{C}_0 \cdot {}^{G_2}\bar{\mathbf{b}}_{2,k} \tag{10}$$

If we have two such bearing measurement pairs (i.e., $k = 0, 1$), we can apply the cross product to yield a third constraint

$$ {}^{G_1}\bar{\mathbf{b}}_{1,0} \times {}^{G_1}\bar{\mathbf{b}}_{1,1} = \mathbf{C}_0({}^{G_2}\bar{\mathbf{b}}_{2,0} \times {}^{G_2}\bar{\mathbf{b}}_{2,1}) \tag{11}$$

Combined, we obtain the matrix equation

$$\begin{aligned} &\begin{bmatrix} {}^{G_1}\bar{\mathbf{b}}_{1,0} & {}^{G_1}\bar{\mathbf{b}}_{1,1} & ({}^{G_1}\bar{\mathbf{b}}_{1,0} \times {}^{G_1}\bar{\mathbf{b}}_{1,1}) \end{bmatrix} \\ &= \mathbf{C}_0 \cdot \begin{bmatrix} -{}^{G_2}\bar{\mathbf{b}}_{2,0} & -{}^{G_2}\bar{\mathbf{b}}_{2,1} & ({}^{G_2}\bar{\mathbf{b}}_{2,0} \times {}^{G_2}\bar{\mathbf{b}}_{2,1}) \end{bmatrix} \end{aligned} \tag{12}$$

and solve for the rotation matrix

$$\begin{aligned} \mathbf{C}_0 = &\begin{bmatrix} {}^{G_1}\bar{\mathbf{b}}_{1,0} & {}^{G_1}\bar{\mathbf{b}}_{1,1} & ({}^{G_1}\bar{\mathbf{b}}_{1,0} \times {}^{G_1}\bar{\mathbf{b}}_{1,1}) \end{bmatrix} \\ &\begin{bmatrix} -{}^{G_2}\bar{\mathbf{b}}_{2,0} & -{}^{G_2}\bar{\mathbf{b}}_{2,1} & ({}^{G_2}\bar{\mathbf{b}}_{2,0} \times {}^{G_2}\bar{\mathbf{b}}_{2,1}) \end{bmatrix}^{-1} \end{aligned} \tag{13}$$

Notice that ${}^{G_2}\bar{\mathbf{b}}_{2,0} \nparallel {}^{G_2}\bar{\mathbf{b}}_{2,1}$ is a necessary and sufficient condition for the matrix inverse to exist, which provides guidance for where to move the robots between measurements.

In the presence of noise, the resulting matrix from (13) might not be a proper rotation matrix, since it is not guaranteed to be orthonormal. A subsequent projection, e.g., using the polar or singular value decomposition [37], would be required to obtain the closest rotation matrix. Further, it is unclear in this formulation how to combine more than two unit vector observations. The above method therefore mostly serves to provide intuition.

The quaternion representation, on the other hand, allows an easy means of combining more than two noisy measurements, and shows that the attitude is unobservable without motion of at least one of the robots. Specifically, using quaternion notation, (10) is written as

$$ \begin{bmatrix} {}^{G_1}\bar{\mathbf{b}}_{1,0} \\ 0 \end{bmatrix} + \bar{q}_0 \otimes \begin{bmatrix} {}^{G_2}\bar{\mathbf{b}}_{2,0} \\ 0 \end{bmatrix} \otimes \bar{q}_0^{-1} = \mathbf{0} \tag{14}$$

We observe that if $\bar{q}_0$ is a particular solution, so is any $\bar{q} = \bar{\alpha} \otimes \bar{q}_0$, if $\bar{\alpha}$ is a quaternion satisfying

$$ \bar{\alpha} \otimes \begin{bmatrix} {}^{G_1}\bar{\mathbf{b}}_{1,0} \\ 0 \end{bmatrix} \otimes \bar{\alpha}^{-1} = \begin{bmatrix} {}^{G_1}\bar{\mathbf{b}}_{1,0} \\ 0 \end{bmatrix} \tag{15}$$

as can be verified by substitution. Notice that (15) holds for any $\bar{\alpha}$ of the form

$$ \bar{\alpha} = \begin{bmatrix} {}^{G_1}\bar{\mathbf{b}}_{1,0} \sin\theta/2 \\ \cos\theta/2 \end{bmatrix}, \quad \theta \in \mathbb{R} $$

which corresponds to a rotation by an arbitrary angle θ about the vector ${}^{G_1}\bar{\mathbf{b}}_{1,0}$. In other words, rotations about the line of sight between the two robots are unobservable.

The quaternion representation also provides an elegant means to obtain a least-squares estimate for the attitude using more than two pairs of bearing measurements. In particular, we want to find the rotation matrix that minimizes the sum of squared errors [see (10)]:

$$\begin{aligned} \mathbf{C}_0 &= \arg\min \sum_k ||{}^{G_1}\bar{\mathbf{b}}_{1,k} + \mathbf{C}_0 \, {}^{G_2}\bar{\mathbf{b}}_{2,k}||^2 \\ &= \arg\min \sum_k \left(||\bar{\mathbf{b}}_{1,k}||^2 + 2 \, {}^{G_1}\bar{\mathbf{b}}_{1,k}^T \, \mathbf{C}_0 \, {}^{G_2}\bar{\mathbf{b}}_{2,k} + ||\bar{\mathbf{b}}_{2,k}||^2 \right) \\ &= \arg\min \sum_k {}^{G_1}\bar{\mathbf{b}}_{1,k}^T \, \mathbf{C}_0 \, {}^{G_2}\bar{\mathbf{b}}_{2,k} \end{aligned} \tag{16}$$

In quaternion representation [see (5) and (9)], this optimization problem is equivalent to

$$\begin{aligned} \bar{q}_0 &= \arg\min \sum_k \begin{bmatrix} {}^{G_1}\bar{\mathbf{b}}_{1,k} \\ 0 \end{bmatrix}^T (\bar{q}_0 \otimes \begin{bmatrix} {}^{G_2}\bar{\mathbf{b}}_{2,k} \\ 0 \end{bmatrix} \otimes \bar{q}_0^{-1}) \\ &= \arg\min \sum_k \begin{bmatrix} {}^{G_1}\bar{\mathbf{b}}_{1,k} \\ 0 \end{bmatrix}^T \mathcal{R}^T(\bar{q}_0) \mathcal{L}(\bar{q}_0) \begin{bmatrix} {}^{G_2}\bar{\mathbf{b}}_{2,k} \\ 0 \end{bmatrix} \\ &= \arg\min \bar{q}_0^T \left(\sum_k \mathcal{L}^T \left(\begin{bmatrix} {}^{G_1}\bar{\mathbf{b}}_{1,k} \\ 0 \end{bmatrix} \right) \mathcal{R} \left(\begin{bmatrix} {}^{G_2}\bar{\mathbf{b}}_{2,k} \\ 0 \end{bmatrix} \right) \right) \bar{q}_0 \end{aligned} \tag{17}$$

The optimal solution is the eigenvector corresponding to the minimum eigenvalue of the matrix $\sum_k \mathcal{L}^T \left(\begin{bmatrix} {}^{G_1}\bar{\mathbf{b}}_{1,k}^T & 0 \end{bmatrix}^T \right) \mathcal{R} \left(\begin{bmatrix} {}^{G_2}\bar{\mathbf{b}}_{2,k}^T & 0 \end{bmatrix}^T \right)$. This solution is analogous to the one derived in [38] for optimal attitude estimation using 3D point correspondences.

Notice that if the robots do not move after the first pair of mutual measurements, the matrix in (17) evaluates to $\mathcal{L}^T \left(\begin{bmatrix} {}^{G_1}\bar{\mathbf{b}}_{1,0}^T & 0 \end{bmatrix}^T \right) \mathcal{R} \left(\begin{bmatrix} {}^{G_2}\bar{\mathbf{b}}_{2,0}^T & 0 \end{bmatrix}^T \right)$. Its characteristic polynomial equals $(\lambda - 1)^2(\lambda + 1)^2$, and hence the minimizer of the quadratic form $\bar{q}_0^T \mathcal{L}^T \left(\begin{bmatrix} {}^{G_1}\bar{\mathbf{b}}_{1,0}^T & 0 \end{bmatrix}^T \right) \mathcal{R} \left(\begin{bmatrix} {}^{G_2}\bar{\mathbf{b}}_{2,0}^T & 0 \end{bmatrix}^T \right) \bar{q}_0$ is not unique. In fact, any minimizer is an element of the 2-dimensional subspace spanned by the two eigenvectors belonging to the double minimum eigenvalue $\lambda = -1$. This confirms our previous statement, that the relative attitude is unobservable unless at least one of the robots moves.

B. Relative Position

In the noise-free case, finding the robots' relative position, $\mathbf{p}_0$, is trivial when both distance and bearing measurements are available. From the first measurement, we have

$$ \mathbf{p}_0 = d_0 \cdot {}^{G_1}\bar{\mathbf{b}}_{1,0} \tag{18}$$

Alternatively, we can use the attitude estimate found in the previous section to solve for the relative position by minimizing a least squares problem. We start by considering the following geometric relations [see Fig. 2(b)]

$$ \mathbf{p}_0 = d_0 \, {}^{G_1}\bar{\mathbf{b}}_{1,0} = \mathbf{p}_{1,k} + d_k \, {}^{G_1}\bar{\mathbf{b}}_{1,k} - \mathbf{C}_0 \mathbf{p}_{2,k} \tag{19}$$

$$ \mathbf{p}_0 = -d_0 \mathbf{C}_0 \, {}^{G_2}\bar{\mathbf{b}}_{2,0} = \mathbf{p}_{1,k} - d_k \mathbf{C}_0 \, {}^{G_2}\bar{\mathbf{b}}_{2,k} - \mathbf{C}_0 \mathbf{p}_{2,k} \tag{20}$$

The translation estimate is found by minimizing the sum of squared errors

$$\mathbf{p}_0 = \arg\min \sum_{k=0}^{n-1} \Bigg(||\mathbf{p}_{1,k} + d_k {}^{G_1}\bar{\mathbf{b}}_{1,k} - \mathbf{C}_0\, \mathbf{p}_{2,k} - \mathbf{p}_0||^2 + ||\mathbf{p}_{1,k} - d_k \mathbf{C}_0 {}^{G_2}\bar{\mathbf{b}}_{2,k} - \mathbf{C}_0 \mathbf{p}_{2,k} - \mathbf{p}_0||^2 \Bigg) \quad (21)$$

Straightforward differentiation yields the solution

$$\mathbf{p}_0 = \frac{1}{2n} \sum_{k=0}^{n-1} \Bigg(\mathbf{p}_{1,k} + d_k {}^{G_1}\bar{\mathbf{b}}_{1,k} - \mathbf{C}_0 \mathbf{p}_{2,k} + \mathbf{p}_{1,k} - d_k \mathbf{C}_0 {}^{G_2}\bar{\mathbf{b}}_{2,k} - \mathbf{C}_0 \mathbf{p}_{2,k} \Bigg) \quad (22)$$

Notice that the above solutions for the relative pose [see (17) and (22)] are suboptimal, since they decouple attitude and position estimation, and do not properly account for measurement noise. A subsequent iterative WLS refinement step (see Sec. VIII) will significantly improve estimation accuracy.

V. 3D Relative Pose from Bearing Measurements

We now consider the case where the two robots measure only relative bearing.

A. Relative Attitude

The computation of the relative attitude in the bearing-only measurement case is identical to that of the range and bearing measurement case (see Section IV-A). Note that no distance information is required in this process.

B. Relative Position

The relative position, however, is more challenging. Our strategy is to first recover the distance between the two global frames, d_0, using the known egomotion and the robot-to-robot bearing measurements. Once d_0 is known, we compute the relative position, $\mathbf{p}_0$, using (18).

Consider again the constraints (19), (20) arising from the geometry shown in Fig. 2(b). Since the relative distances d_k are unknown, we eliminate these by forming the cross product with the unit vectors ${}^{G_1}\bar{\mathbf{b}}_{1,k}$ and ${}^{G_2}\bar{\mathbf{b}}_{2,k}$, respectively.

$$d_0 \lfloor {}^{G_1}\bar{\mathbf{b}}_{1,k} \times \rfloor {}^{G_1}\bar{\mathbf{b}}_{1,0} = \lfloor {}^{G_1}\bar{\mathbf{b}}_{1,k} \times \rfloor (\mathbf{p}_{1,k} - \mathbf{C}_0 \mathbf{p}_{2,k}) \quad (23)$$

$$-d_0 \lfloor {}^{G_2}\bar{\mathbf{b}}_{2,k} \times \rfloor {}^{G_2}\bar{\mathbf{b}}_{2,0} = \lfloor {}^{G_2}\bar{\mathbf{b}}_{2,k} \times \rfloor (\mathbf{C}_0^T \mathbf{p}_{1,k} - \mathbf{p}_{2,k}) \quad (24)$$

The distance estimate is found by minimizing the sum of squared errors

$$d_0 = \arg\min \sum_{k=1}^{n-1} \Big(||d_0 \lfloor {}^{G_1}\bar{\mathbf{b}}_{1,k} \times \rfloor {}^{G_1}\bar{\mathbf{b}}_{1,0} - \lfloor {}^{G_1}\bar{\mathbf{b}}_{1,k} \times \rfloor (\mathbf{p}_{1,k} - \mathbf{C}_0 \mathbf{p}_{2,k})||^2 + ||d_0 \lfloor {}^{G_2}\bar{\mathbf{b}}_{2,k} \times \rfloor {}^{G_2}\bar{\mathbf{b}}_{2,0} + \lfloor {}^{G_2}\bar{\mathbf{b}}_{2,k} \times \rfloor (\mathbf{C}_0^T \mathbf{p}_{1,k} - \mathbf{p}_{2,k})||^2 \Big) \quad (25)$$

Differentiating this last expression with respect to d_0 and setting it equal to zero yields

$$d_0 = \frac{\sum_{k=1}^{n-1} (\mathbf{p}_{1,k} - \mathbf{C}_0 \mathbf{p}_{2,k})^T (\lfloor {}^{G_1}\bar{\mathbf{b}}_{1,k} \times \rfloor^2 {}^{G_1}\bar{\mathbf{b}}_{1,0} - \mathbf{C}_0 \lfloor {}^{G_2}\bar{\mathbf{b}}_{2,k} \times \rfloor^2 {}^{G_2}\bar{\mathbf{b}}_{2,0})}{\sum_{k=1}^{n-1} \left({}^{G_1}\bar{\mathbf{b}}_{1,0}^T \lfloor {}^{G_1}\bar{\mathbf{b}}_{1,k} \times \rfloor^2 {}^{G_1}\bar{\mathbf{b}}_{1,0} + {}^{G_2}\bar{\mathbf{b}}_{2,0}^T \lfloor {}^{G_2}\bar{\mathbf{b}}_{2,k} \times \rfloor^2 {}^{G_2}\bar{\mathbf{b}}_{2,0} \right)} \quad (26)$$

As noted before, this solution is not optimal from an estimation-theoretic point of view, but will provide a good initial estimate for a subsequent iterative WLS refinement.

VI. 3D Relative Pose From Distance Measurements

When only inter-robot distance measurements are available, the problem of determining the transformation between the global frames is most challenging.

From the first distance measurement d_0, we know that the position of robot R_2 lies on a sphere that satisfies the following equation

$$d_0^2 = \mathbf{p}_0^T \mathbf{p}_0 \quad (27)$$

Generally, the inter-robot distance is given by the 2-norm of vector $\mathbf{p}_k$ connecting the positions of robots R_1 and R_2 at time k (see Fig. 2), i.e.,

$$d_k = ||\mathbf{p}_k||_2 \,, \quad k = 1, \ldots, n-1 \quad (28)$$

where

$$\mathbf{p}_k = \mathbf{C}_{1,k} \left(\mathbf{p}_0 + \mathbf{C}_0\, \mathbf{p}_{2,k} - \mathbf{p}_{1,k} \right) \quad (29)$$

Squaring both sides of (28) and substituting (29) and (27) yields the following constraints

$$\begin{aligned} d_k^2 &= (\mathbf{p}_0 + \mathbf{C}_0\, \mathbf{p}_{2,k} - \mathbf{p}_{1,k})^T (\mathbf{p}_0 + \mathbf{C}_0\, \mathbf{p}_{2,k} - \mathbf{p}_{1,k}) \\ \Leftrightarrow \varepsilon_k &= (\mathbf{p}_{1,k} - \mathbf{p}_0)^T \mathbf{C}_0\, \mathbf{p}_{2,k} + \mathbf{p}_{1,k}^T \mathbf{p}_0 \end{aligned} \quad (30)$$

where, for brevity, $\varepsilon_k := \frac{1}{2}(d_0^2 + \mathbf{p}_{1,k}^T \mathbf{p}_{1,k} + \mathbf{p}_{2,k}^T \mathbf{p}_{2,k} - d_k^2)$ is a function of quantities that are either measured or estimated and therefore known.

We combine all constraints (1), (27), and (30) as

$$\bar{q}^T \bar{q} = 1 \quad (31)$$

$$\mathbf{p}_0^T \mathbf{p}_0 = d_0^2 \quad (32)$$

$$(\mathbf{p}_{1,k} - \mathbf{p}_0)^T \mathbf{C}_0\, \mathbf{p}_{2,k} + \mathbf{p}_{1,k}^T \mathbf{p}_0 = \varepsilon_k, \; k = 1, \ldots, n-1 \quad (33)$$

Notice that the constraints (33) are cubic in the unknown elements of $\mathbf{p}_0$ and $\bar{q}_0$, since the rotation matrix $\mathbf{C}$ is quadratic in the quaternion elements [see (2)].

From research in parallel manipulators [39] it is known that, given six distance measurements, this polynomial system has 40 solutions. There exist algorithms to find all 40 solutions based on successively eliminating variables from the system of polynomial equations and solving the univariate 40^{th}-order polynomial [33], [34], [40]. All of these elimination approaches are very sensitive to numerical errors, and hence require non-standard floating-point data types with a high number of significant digits (e.g., 30 digits of accuracy is required for the method reported in [34]).

Alternatively, purely numerical algorithms based on homotopy continuation, such as PHCpack [41], yield very accurate solutions, and have been successfully applied to solve the forward kinematics of the Stewart-Gough mechanism. Unfortunately, in our experiments, PHCpack required 25 seconds to solve one instance of this problem, a prohibitive delay for many robotic applications. Further difficulties arise in the presence of noise, or when more than six measurements become available, since even slight perturbations in the data can cause this system to have no solution.

Less complicated, closed-form algorithms can be obtained by imposing strong additional constraints on the geometry of the system (or, in our case, the trajectories of the robots), and by adding additional sensor measurements. One example is the work by Bonev and Ryu [42] that requires a planar platform (i.e., planar trajectory of robot R_2), and a total of 9 distance measurements.

In what follows, we will present an efficient algorithm that uses 10 distance measurements and determines the unique solution in closed form, without any constraints on the system geometry. Before presenting the algorithm, we first provide an argument that 10 measurements will actually suffice to determine a unique solution.

A. Uniqueness Argument

We know that given six distance measurements, the square polynomial system (31)-(33) has 40 solutions. Distinguishing the unique solution that corresponds to the true relative pose of the robots requires additional measurements. This process adds extra constraints in the form of (33) to the polynomial system, which eliminate the spurious solutions obtained from the square system. The question that needs to be answered is how many additional measurements are required to eliminate all but the true solution. We will argue, that for generic robot trajectories, with probability 1 only one additional measurement suffices to identify the unique solution.

To verify this, consider the case where after processing six distance measurements, 40 solutions are found, denoted as $\mathbf{x}_i = [\mathbf{p}_0^T,\ \bar{q}_0^T]^T,\ i = 1, \ldots, 40$. Without loss of generality, we first assume that $\mathbf{x}_1$ corresponds to the true inter-robot transformation. Immediately after, the robots move to their new positions, $\mathbf{p}_{1,6}$ and $\mathbf{p}_{2,6}$ respectively, and record the 7^{th} distance measurement d_6. Then the true inter-robot transformation $\mathbf{x}_1$ should also satisfy (33) for $k = 6$:

$$(\mathbf{p}_{1,6} - \mathbf{p}_0)^T \mathbf{C}_0\ \mathbf{p}_{2,6} + \mathbf{p}_{1,6}^T \mathbf{p}_0 - \varepsilon_6 = 0 \Leftrightarrow g(\mathbf{x}_1, \boldsymbol{\vartheta}) = 0 \tag{34}$$

where $\boldsymbol{\vartheta} = [\mathbf{p}_{1,6}^T,\ \mathbf{p}_{2,6}^T,\ d_6]^T$. Given $\mathbf{x}_1$, we denote by $\mathcal{V}_1$ the set of all values of $\boldsymbol{\vartheta}$ that satisfy (34). Note that $\mathcal{V}_1$ is a 6-dimensional variety, which implies that the two robots can move to any position in 3D.

If we now assume that there exists a second solution, for example $\mathbf{x}_2$, then it should also satisfy (34), i.e.,

$$g(\mathbf{x}_2, \boldsymbol{\vartheta}) = 0 \tag{35}$$

As before, given $\mathbf{x}_2$, we denote by $\mathcal{V}_2$ the set of all values of $\boldsymbol{\vartheta}$ that satisfy (35).

In the event that both $\mathbf{x}_1$ and $\mathbf{x}_2$ are valid solutions, then $\boldsymbol{\vartheta}$ – which is the realization of the robots' displacement estimates and distance measurement – must satisfy (34) *and* (35), and thus $\boldsymbol{\vartheta}$ belongs to the set $\mathcal{V} = \mathcal{V}_1 \cap \mathcal{V}_2$. Note that since $\mathcal{V}$ is constrained by an additional equation [see (35)], $\mathcal{V} \subset \mathcal{V}_1$, and the dimension of $\mathcal{V}$ is smaller than that of $\mathcal{V}_1$ [43, Thm. 3, Ch. 9, Sec. 4]. Hence, the probability that the robots' displacements are such that two solutions exist, is $|\mathcal{V}|/|\mathcal{V}_1|$, which is zero[2]. Following the same process, one can show that the probability of the event that more than two solutions exist is also zero.

Therefore, we conclude that with probability 1, for generic robot trajectories, seven distance measurements are sufficient to obtain a unique solution.

B. Algebraic Method

We hereafter present an algebraic method for determining the unique relative pose between the two robots from at least 10 distance measurements.

The key idea behind this approach is to introduce the new variable $\mathbf{r}_0 := \mathbf{C}_0^T \mathbf{p}_0$, which allows us to reduce the order of the polynomial system from cubic to quadratic, at the cost of an increased number of unknowns. The resulting system can then be solved using lifting (Veronese mapping)[3].

Using the new variable $\mathbf{r}_0$, we can rewrite (33) as

$$\mathbf{p}_{1,k}^T \mathbf{C}_0\, \mathbf{p}_{2,k} + \mathbf{p}_{1,k}^T \mathbf{p}_0 - \mathbf{p}_{2,k}^T \mathbf{r}_0 - \varepsilon_k = 0,\ k = 1, \ldots, n-1 \tag{36}$$

This system of equations, as well as the quaternion unit norm constraint (31) is quadratic *only* in the elements of $\bar{q}_0$. However, we can treat it as a *linear* system of equations by introducing new variables for the ten quadratic monomials $q_i q_j,\ i, j = 1, \ldots, 4,\ i \geq j$. Specifically, we stack these monomials in a vector $\bar{\mathbf{q}} = \begin{bmatrix} q_{11} & q_{12} & \ldots & q_{44} \end{bmatrix}^T_{10\times 1}$, where $q_{ij} := q_i q_j$, and rewrite (31) and (36) as the following homogeneous linear system

$$\mathbf{M}\bar{\mathbf{q}} + \mathbf{A} \begin{bmatrix} \mathbf{p}_0 \\ \mathbf{r}_0 \end{bmatrix} - \boldsymbol{\varepsilon} = 0 \Rightarrow \mathcal{M}\bar{\mathbf{x}} = \mathbf{0} \tag{37}$$

where

$$\mathbf{A} := \begin{bmatrix} \mathbf{p}_{1,1}^T & -\mathbf{p}_{2,1}^T \\ \vdots & \vdots \\ \mathbf{p}_{1,n-1}^T & -\mathbf{p}_{2,n-1}^T \\ \mathbf{0} & \mathbf{0} \end{bmatrix}, \quad \boldsymbol{\varepsilon} := \begin{bmatrix} \varepsilon_1 \\ \vdots \\ \varepsilon_{n-1} \\ 1 \end{bmatrix} \tag{38}$$

$$\mathcal{M} := \begin{bmatrix} \mathbf{M} & \mathbf{A} & -\boldsymbol{\varepsilon} \end{bmatrix}$$
$$\bar{\mathbf{x}} := \begin{bmatrix} \bar{\mathbf{q}}^T & \mathbf{p}_0^T & \mathbf{r}_0^T & \rho \end{bmatrix}^T \tag{39}$$

The first $n-1$ rows of $\mathbf{M}$ are constructed from the elements of $\mathbf{p}_{1,k}^T \mathbf{C}_0\, \mathbf{p}_{2,k}$. Specifically, if we denote $\mathbf{p}_{2,k} = \begin{bmatrix} x_{2,k} & y_{2,k} & z_{2,k} \end{bmatrix}^T$, substitute from (2), and rearrange the resulting terms, we obtain the following expression for the k-th row of $\mathbf{M}$

$$\mathbf{M}(k,:) = \mathbf{p}_{1,k}^T \begin{bmatrix} x_{2,k} & 2y_{2,k} & 2z_{2,k} & 0 & -x_{2,k} \\ -y_{2,k} & 2x_{2,k} & 0 & 2z_{2,k} & y_{2,k} \\ -z_{2,k} & 0 & 2x_{2,k} & -2y_{2,k} & -z_{2,k} \end{bmatrix}$$
$$\begin{bmatrix} 0 & -2z_{2,k} & -x_{2,k} & 2y_{2,k} & x_{2,k} \\ 2z_{2,k} & 0 & -y_{2,k} & -2x_{2,k} & y_{2,k} \\ 2y_{2,k} & 2x_{2,k} & z_{2,k} & 0 & z_{2,k} \end{bmatrix}, k = 1, \ldots, n-1 \tag{40}$$

[2] $|\cdot|$ is a measure of the size of a set. When the set is continuous, it is the total volume of the set.

[3] Similar techniques have been used in the computer vision literature for solving the relative pose problem for two cameras from point or line correspondences [44], [45].

The last row of $\mathcal{M}$ corresponds to the unit quaternion constraint (31), where

$$\mathbf{M}(n,:) = \begin{bmatrix} 1 & 0 & 0 & 0 & 1 & 0 & 0 & 1 & 0 & 1 \end{bmatrix} \tag{41}$$

The vector of unknowns, $\bar{\mathbf{x}}_{17\times 1}$, is a concatenation of the vector $\bar{\mathbf{q}}$, the position vectors $\mathbf{p}_0$ and $\mathbf{r}_0$, and a scalar, ρ, which we will later constrain to $\rho = 1$. Notice that if $\bar{\mathbf{x}}$ is uniquely specified, this in turn uniquely determines the relative pose $\mathbf{p}_0$ and $\bar{q}_0$. The relative position, $\mathbf{p}_0$, can be read directly from $\bar{\mathbf{x}}$, and the elements of $\bar{q}_0$ can be extracted from $\bar{\mathbf{q}}$ using the convention that $q_4 \geq 0$ (which holds without loss of generality, since $\bar{q}_0$ and $-\bar{q}_0$ correspond to the same rotation [35]). The elements of $\bar{q}_0$ can be extracted from $\bar{\mathbf{q}}$ by setting $q_i = \sqrt{q_{ii}},\ i = 1,\ldots,4$, with the choice of positive q_4 uniquely determining the sign for the remaining q_i by $\mathrm{sgn}(q_i) = \mathrm{sgn}(q_{i4})$.

The unknown vector $\bar{\mathbf{x}}$ will lie in the nullspace of $\mathcal{M}_{n\times 17}$, or $\bar{\mathbf{x}} \in \ker(\mathcal{M})$. Letting $\boldsymbol{\mu}_i,\ i = 1,\ldots,N$ denote the N orthonormal basis vectors of $\ker(\mathcal{M})_{17\times N}$, where $N \geq 17-n$, we can therefore write

$$\bar{\mathbf{x}} = \sum_{i=1}^{N} \lambda_i \boldsymbol{\mu}_i \tag{42}$$

Notice that a given set of λ_i uniquely defines $\bar{\mathbf{x}}$, and hence the relative pose. Ideally, we would want a one-dimensional nullspace, since then $\bar{\mathbf{x}}$ would follow immediately from the constraint $\rho = 1$. However, using only (37), this would require at least $n = 16$ distance measurements. With fewer distance measurements, so that the nullspace of $\mathcal{M}$ is of dimension $N > 1$, we need to impose additional constraints on the λ_i's, as we outline next.

We will restrict ourselves to *homogeneous, quadratic* constraints in the elements $x_k,\ k = 1,\ldots,17$ of $\bar{\mathbf{x}}$. Substituting the appropriate row-elements of (42), we can write such constraints as

$$\begin{aligned} & x_k x_l = x_{k'} x_{l'} \\ \Leftrightarrow & (\sum_{i=1}^{N} \lambda_i \mu_{ik})(\sum_{j=1}^{N} \lambda_j \mu_{jl}) = (\sum_{i=1}^{N} \lambda_i \mu_{ik'})(\sum_{j=1}^{N} \lambda_j \mu_{jl'}) \\ \Leftrightarrow & \sum_{i=1}^{N} \lambda_i^2 (\mu_{ik}\mu_{il} - \mu_{ik'}\mu_{il'}) + \\ & \sum_{i=1}^{N} \sum_{j=i+1}^{N} \lambda_i \lambda_j (\mu_{ik}\mu_{jl} + \mu_{il}\mu_{jk} - \mu_{ik'}\mu_{jl'} - \mu_{il'}\mu_{jk'}) = 0 \end{aligned} \tag{43}$$

where μ_{ik} denotes the k-th element of the vector $\boldsymbol{\mu}_i$.

For the elements of $\bar{\mathbf{q}}$, 20 such quadratic constraints can be established (see Appendix), another six constraints are derived from the rows of $\mathbf{p}_0 = \mathbf{C}_0\,\mathbf{r}_0$ and $\mathbf{r}_0 = \mathbf{C}_0^T\,\mathbf{p}_0$, and finally one constraint from $\mathbf{p}_0^T\,\mathbf{p}_0 = d_0^2$, giving a total of 27 *linearly (but not necessarily algebraically) independent* constraints. Notice that the final 7 equations can be written as a homogeneous, quadratic constraint in the elements of $\bar{\mathbf{x}}$ by exploiting the fact that $\rho = \rho^2 = 1$.

Similarly to the linearization of the quadratic equations in the elements of $\bar{q}_0$, we can express these 27 constraints as a homogeneous system of linear equations in the variables $\bar{\boldsymbol{\lambda}} := \begin{bmatrix} \lambda_{11} & \lambda_{12} & \ldots & \lambda_{NN} \end{bmatrix}^T$, with $\lambda_{ij} := \lambda_i \lambda_j$, as

$$\mathcal{L}\bar{\boldsymbol{\lambda}} = \mathbf{0} \tag{44}$$

The elements of matrix $\mathcal{L}$ are functions only of the known null vectors $\boldsymbol{\mu}_i, i = 1,\ldots,N$. Notice that the dimension of $\bar{\boldsymbol{\lambda}}$ depends on the dimension N of $\ker(\mathcal{M})$, as $\dim(\bar{\boldsymbol{\lambda}}) = \frac{N(N+1)}{2}$. In order for (44) to have a unique solution, $\mathcal{L}$ must be rank-deficient by exactly one. For this reason, the 27 constraints mentioned above will only be able to uniquely specify $\bar{\boldsymbol{\lambda}}$ for $N \leq 7$, in turn requiring $n \geq 10$ distance measurements.

Choosing $\bar{\boldsymbol{\lambda}}$ as the nullvector of $\mathcal{L}$ (or, in the presence of noise, the singular vector corresponding to the smallest singular value), we can recover the λ_i's up to scale from the elements of $\bar{\boldsymbol{\lambda}}$ by setting $\lambda_i = \sqrt{\lambda_{ii}}$, with the choice of sign for λ_1 determining the sign for the remaining λ_i from the elements of $\bar{\boldsymbol{\lambda}}$, i.e., $\mathrm{sgn}(\lambda_i) = \mathrm{sgn}(\lambda_1)\mathrm{sgn}(\lambda_{1i})$. Additionally, we enforce the correct scale of $\bar{\boldsymbol{\lambda}}$ from the constraint

$$\rho = \sum_{i=1}^{N} \lambda_i \mu_{i,17} = 1 \tag{45}$$

using the last row of (42).

Once the coefficients λ_i have been determined, the vector $\bar{\mathbf{x}}$ is computed using (42). Finally, the relative pose, $(\mathbf{p}_0,\, \bar{q}_0)$, is reconstructed as outlined above.

A necessary condition for this method to work is that the nullspace of $\mathcal{M}$ is of dimension $N \leq 7$, and the nullspace of $\mathcal{L}$ is of dimension 1. Singular configurations (in which one or more degrees of freedom are unobservable from the given measurements) will manifest themselves in the form of matrices $\mathcal{M}$ and $\mathcal{L}$ losing rank. Our algorithm is able to detect such pathological cases, and will require more distance measurements to be taken before a solution is computed.

In the next section, we analyze the observability properties of the system using a continuous-time kinematic model, and show that the robot-to-robot relative pose is locally weakly observable for all three cases of distance and bearing, bearing-only, and distance-only measurements.

VII. Observability Analysis

It is essential to investigate the observability of a system when designing estimators. A system is called *observable* if its state at a certain time instant can be uniquely determined given a finite sequence of its outputs [46]. Intuitively this means that the measurements of an observable system provide sufficient information for estimating its state. In contrast, the state vector of unobservable systems cannot be recovered regardless of the duration of the estimation process.

The system describing the 6 d.o.f. robot-to-robot transformation is nonlinear. Therefore, tests designed for *linear time-invariant* systems (e.g., the rank of the Gramian matrix [47] or the Popov-Belevitch-Hautus (PBH) test [48]) cannot be used for examining its observability properties. Instead, we hereafter employ the observability rank condition based on Lie derivatives [49].

In particular, we study the observability of the time-varying relative pose $\mathbf{p}_t := {}^{R_{1,t}}\mathbf{p}_{R_{2,t}}$, $\mathbf{C}_t := {}^{R_{1,t}}_{R_{2,t}}\mathbf{C}$ in a continuous-time formulation, with linear and rotational velocities, $\mathbf{v}$

and $\boldsymbol{\omega}$, as control inputs. Following a brief review of Lie derivatives and the observability rank condition, as well as the continuous-time system formulation of the relative pose problem, we provide sufficient conditions for observability when using distance and bearing (Section VII-C1), bearing-only (Section VII-C2), and distance-only measurements (Section VII-C3).

A. Nonlinear Observability

Consider the state-space representation of the following general, nonlinear system:

$$\begin{cases} \dot{\mathbf{x}} = \mathbf{f}(\mathbf{x}, \mathbf{u}) \\ \mathbf{y} = \mathbf{h}(\mathbf{x}) \end{cases} \tag{46}$$

where $\mathbf{x} \in \mathbb{R}^n$ is the state vector, $\mathbf{u} = [u_1 \ \dots \ u_l]^T \in \mathbb{R}^l$ is the vector of control inputs, and $\mathbf{y} = [y_1 \ \dots \ y_m]^T \in \mathbb{R}^m$ is the measurement vector, with $y_k = h_k(\mathbf{x})$, $k = 1, \dots, m$.

We consider the special case of (46), where the process function, $\mathbf{f}$, can be separated into a summation of functions, each one excited by a different component of the control input vector, i.e., (46) can be written as:

$$\begin{cases} \dot{\mathbf{x}} = \mathbf{f}_0(\mathbf{x}) + \mathbf{f}_1(\mathbf{x})u_1 + \cdots + \mathbf{f}_l(\mathbf{x})u_l \\ \mathbf{y} = \mathbf{h}(\mathbf{x}) \end{cases} \tag{47}$$

where $\mathbf{f}_0$ is the zero-input segment of the process model, and $\mathbf{f}_i(\mathbf{x}) = [f_{i1}(\mathbf{x}) \ \dots \ f_{in}(\mathbf{x})]^T$.

Lie derivatives quantify the impact of changes in the control input on the output functions. The zeroth-order Lie derivative of any (scalar) function is defined as the function itself, i.e., $\mathfrak{L}^0 h_k(\mathbf{x}) = h_k(\mathbf{x})$. The first-order Lie derivative of function $h_k(\mathbf{x})$ with respect to $\mathbf{f}_i$ is defined as:

$$\begin{aligned} \mathfrak{L}^1_{\mathbf{f}_i} h_k(\mathbf{x}) &= \frac{\partial h_k(\mathbf{x})}{\partial x_1} f_{i1}(\mathbf{x}) + \cdots + \frac{\partial h_k(\mathbf{x})}{\partial x_n} f_{in}(\mathbf{x}) \\ &= \nabla h_k(\mathbf{x}) \cdot \mathbf{f}_i(\mathbf{x}) \end{aligned} \tag{48}$$

Considering that $\mathfrak{L}^1_{\mathbf{f}_i} h_k(\mathbf{x})$ is a scalar function itself, the second-order Lie derivative of $h_k(\mathbf{x})$ with respect to $\mathbf{f}_i$ is defined recursively:

$$\mathfrak{L}^2_{\mathbf{f}_i} h_k(\mathbf{x}) = \mathfrak{L}^1_{\mathbf{f}_i} \left(\mathfrak{L}^1_{\mathbf{f}_i} h_k(\mathbf{x}) \right) = \nabla \mathfrak{L}^1_{\mathbf{f}_i} h_k(\mathbf{x}) \cdot \mathbf{f}_i(\mathbf{x}) \tag{49}$$

Higher-order Lie derivatives are computed similarly. Additionally, it is possible to define mixed Lie derivatives with respect to different functions of the process model. For example, the second-order Lie derivative of h_k with respect to $\mathbf{f}_j$ and $\mathbf{f}_i$ is:

$$\mathfrak{L}^2_{\mathbf{f}_j \mathbf{f}_i} h_k(\mathbf{x}) = \mathfrak{L}^1_{\mathbf{f}_j} \left(\mathfrak{L}^1_{\mathbf{f}_i} h_k(\mathbf{x}) \right) = \nabla \mathfrak{L}^1_{\mathbf{f}_i} h_k(\mathbf{x}) \cdot \mathbf{f}_j(\mathbf{x}) \tag{50}$$

Based on the preceding expressions for the Lie derivatives, the observability matrix is defined as the matrix with rows:

$$\mathcal{O} \triangleq \{ \nabla \mathfrak{L}^\ell_{\mathbf{f}_i \cdots \mathbf{f}_j} h_k(\mathbf{x}) \mid i, j = 0, \dots, l; k = 1, \dots, m; \ell \in \mathbb{N} \} \tag{51}$$

The important role of this matrix in the observability analysis of a nonlinear system is captured by Theorem 3.1 in [49], repeated below:

Definition 1 (Observability Rank Condition): The observability rank condition is satisfied when the observability matrix (51) is full rank.

Theorem 1 (Observability Sufficient Condition): If a system satisfies the observability rank condition then it is locally weakly observable.

Theorem 1 will be used in the following sections to determine the sufficient conditions for observability.

B. Continuous-time Kinematic Model

In this section, we derive the continuous-time kinematic model employed in the 3D robot-to-robot relative pose. Consider again the geometry shown in Fig. 2. Notice that the transformation between the two global frames, $\{G_1\}$ and $\{G_2\}$, is *constant*, causing the time-derivative of their relative position and orientation to vanish, i.e., $\dot{\mathbf{p}}_0 = \mathbf{0}$, $\dot{\bar{q}}_0 = \mathbf{0}$. In order to be able to use the framework of Section VII-A, we will instead analyze the observability of the time-varying *local* 6 d.o.f. transformation between the robots, namely the translation $\mathbf{p}_t := {}^{R_{1,t}}\mathbf{p}_{R_{2,t}}$ and rotation $\mathbf{C}_t := {}^{R_{1,t}}_{R_{2,t}}\mathbf{C}$, or the corresponding quaternion $\bar{q}_t$.

We start with the continuous-time version of (29) (changing the subscript k to t to denote continuous time).

$$\mathbf{p}_t = \mathbf{C}_{1,t}(\mathbf{p}_0 + \mathbf{C}_0 \, \mathbf{p}_{2,t} - \mathbf{p}_{1,t}) \tag{52}$$

Taking derivatives with respect to time, and exploiting the constant global transformation, we have

$$\dot{\mathbf{p}}_t = \dot{\mathbf{C}}_{1,t}(\mathbf{p}_0 + \mathbf{C}_0 \, \mathbf{p}_{2,t} - \mathbf{p}_{1,t}) + \mathbf{C}_{1,t}(\mathbf{C}_0 \dot{\mathbf{p}}_{2,t} - \dot{\mathbf{p}}_{1,t}) \tag{53}$$

Using the relationship $\dot{\mathbf{C}}_{1,t} = -\lfloor \boldsymbol{\omega}_1 \times \rfloor \mathbf{C}_{1,t}$, the expression for $\mathbf{p}_t$ from (52), and introducing the robots' linear and rotational velocities, $\mathbf{v}_i$ and $\boldsymbol{\omega}_i$, $i = 1, 2$ expressed with respect to their local frames so that $\dot{\mathbf{p}}_{1,t} = \mathbf{C}^T_{1,t}\mathbf{v}_1$, and $\dot{\mathbf{p}}_{2,t} = \mathbf{C}^T_{2,t}\mathbf{v}_2$, we obtain

$$\begin{aligned} \dot{\mathbf{p}}_t &= -\lfloor \boldsymbol{\omega}_1 \times \rfloor \mathbf{p}_t + \mathbf{C}_{1,t}(\mathbf{C}_0 \mathbf{C}^T_{2,t}\mathbf{v}_2 - \mathbf{C}^T_{1,t}\mathbf{v}_1) \\ &= \lfloor \mathbf{p}_t \times \rfloor \boldsymbol{\omega}_1 + \mathbf{C}_t \mathbf{v}_2 - \mathbf{v}_1 \end{aligned} \tag{54}$$

We derive the kinematic model for the relative orientation in a similar fashion using the quaternion representation of rotations.

$$\bar{q}_t = \bar{q}_{1,t} \otimes \bar{q}_0 \otimes \bar{q}^{-1}_{2,t}$$

Again taking derivatives with respect to time, we obtain:

$$\begin{aligned} \dot{\bar{q}}_t &= \dot{\bar{q}}_{1,t} \otimes \bar{q}_0 \otimes \bar{q}^{-1}_{2,t} + \bar{q}_{1,t} \otimes \bar{q}_0 \otimes \dot{\bar{q}}^{-1}_{2,t} \\ &= \frac{1}{2} \begin{bmatrix} \boldsymbol{\omega}_1 \\ 0 \end{bmatrix} \otimes \bar{q}_t - \bar{q}_t \otimes \frac{1}{2} \begin{bmatrix} \boldsymbol{\omega}_2 \\ 0 \end{bmatrix} \\ &= \frac{1}{2} \boldsymbol{\Xi}(\bar{q}_t) \boldsymbol{\omega}_1 - \frac{1}{2} \boldsymbol{\Psi}(\bar{q}_t) \boldsymbol{\omega}_2 \end{aligned} \tag{55}$$

where we have used the relationships $\dot{\bar{q}}_{1,t} = \frac{1}{2} \begin{bmatrix} \boldsymbol{\omega}_1 \\ 0 \end{bmatrix} \otimes \bar{q}_{1,t}$, and $\dot{\bar{q}}^{-1}_{2,t} = -\frac{1}{2} \bar{q}^{-1}_{2,t} \otimes \begin{bmatrix} \boldsymbol{\omega}_2 \\ 0 \end{bmatrix}$ (see [36]). From here on, we will omit the subscript t to simplify the notation.

In order to compute the Lie derivatives, we rewrite the nonlinear kinematic model [see (54) and (55)] as:

$$\underbrace{\begin{bmatrix}\dot{\mathbf{p}}\\ \dot{\bar{q}}\end{bmatrix}}_{\dot{\mathbf{x}}} = \underbrace{\begin{bmatrix}-\mathbf{I}_3\\ \mathbf{0}_{4\times 3}\end{bmatrix}}_{\mathbf{f}_1}\mathbf{v}_1 + \underbrace{\begin{bmatrix}\mathbf{C}\\ \mathbf{0}_{4\times 3}\end{bmatrix}}_{\mathbf{f}_2}\mathbf{v}_2 + \underbrace{\begin{bmatrix}\lfloor \mathbf{p}\times \rfloor\\ \frac{1}{2}\boldsymbol{\Xi}(\bar{q})\end{bmatrix}}_{\mathbf{f}_3}\boldsymbol{\omega}_1 + \underbrace{\begin{bmatrix}\mathbf{0}_{3\times 3}\\ -\frac{1}{2}\boldsymbol{\Psi}(\bar{q})\end{bmatrix}}_{\mathbf{f}_4}\boldsymbol{\omega}_2 \tag{56}$$

C. Observability of the 3D Robot-to-Robot Relative Pose

1) Distance and bearing measurements: When both distance and bearing measurements are available, we can equivalently use a measurement model that directly measures the relative position.

$$\mathbf{h}(\mathbf{x}) = \mathbf{p} \tag{57}$$

We hereafter compute the necessary Lie derivatives of $\mathbf{h}$ and their gradients.

- *Zeroth-order Lie derivative* ($\mathfrak{L}^0\mathbf{h}$) The zeroth-order Lie derivative of a function is the function itself, i.e.,

  $$\mathfrak{L}^0\mathbf{h} = \mathbf{h} = \mathbf{p}$$

  Hence, the gradient of the zeroth-order Lie derivative is

  $$\nabla\mathfrak{L}^0\mathbf{h} = \begin{bmatrix}\mathbf{I}_3 & \mathbf{0}_{3\times 4}\end{bmatrix} \tag{58}$$

- *First-order Lie derivative* ($\mathfrak{L}^1_{\mathbf{f}_2}\mathbf{h}$)

  $$\mathfrak{L}^1_{\mathbf{f}_2}\mathbf{h} = \nabla\mathfrak{L}^0\mathbf{h}\cdot\mathbf{f}_2 = \mathbf{C} \tag{59}$$

  We stack the columns of $\mathbf{C}$ to form a 9×1 vector and take its gradient with respect to $\bar{q}$ (we omit its gradient with respect to the position part $\mathbf{p}$, since it is zero):

  $$\nabla_{\bar{q}}\mathfrak{L}^1_{\mathbf{f}_2}\mathbf{h} = 2\begin{bmatrix} q_1 & -q_2 & -q_3 & q_4\\ q_2 & q_1 & -q_4 & -q_3\\ q_3 & q_4 & q_1 & q_2\\ q_2 & q_1 & q_4 & q_3\\ -q_1 & q_2 & -q_3 & q_4\\ -q_4 & q_3 & q_2 & -q_1\\ q_3 & -q_4 & q_1 & -q_2\\ q_4 & q_3 & q_2 & q_1\\ -q_1 & -q_2 & q_3 & q_4\end{bmatrix} \tag{60}$$

Note that $\nabla_{\bar{q}}\mathfrak{L}^1_{\mathbf{f}_2}\mathbf{h}$ has full column rank, since the determinant of $(\nabla_{\bar{q}}\mathfrak{L}^1_{\mathbf{f}_2}\mathbf{h})^T(\nabla_{\bar{q}}\mathfrak{L}^1_{\mathbf{f}_2}\mathbf{h})$ is nonzero, i.e.,

$$\det[(\nabla_{\bar{q}}\mathfrak{L}^1_{\mathbf{f}_2}\mathbf{h})^T(\nabla_{\bar{q}}\mathfrak{L}^1_{\mathbf{f}_2}\mathbf{h})] = 6144(q_1^2+q_2^2+q_3^2+q_4^2)^4$$

At this point, we are ready to present the main result of the observability analysis of the system (56) with distance and bearing measurements (57):

Lemma 1: Given distance and bearing measurements, a sufficient condition for the system described by (56) and (57) to be locally weakly observable is $\mathbf{v}_2 \neq \mathbf{0}$.

Proof: Using (58) and (60), we construct the following observability matrix

$$\mathcal{O}_1 = \begin{bmatrix}\nabla\mathfrak{L}^0\mathbf{h}\\ \nabla\mathfrak{L}^1_{\mathbf{f}_2}\mathbf{h}\end{bmatrix} = \begin{bmatrix}\mathbf{I}_3 & \mathbf{0}_{3\times 4}\\ \mathbf{0}_{9\times 3} & \nabla_{\bar{q}}\mathfrak{L}^1_{\mathbf{f}_2}\mathbf{h}\end{bmatrix} \tag{61}$$

which is full rank. Therefore the observability rank condition is satisfied and, from Theorem 1, the system is locally weakly observable. ■

2) Bearing-only measurements: To proceed with the observability analysis for bearing-only measurements, we first consider the case where only one robot (we choose robot R_1) is equipped with a bearing sensor. We will show that this system is locally weakly observable. To simplify the derivation, we employ the standard pinhole camera model, i.e.,

$$\mathbf{h}(\mathbf{x}) = \begin{bmatrix} x/z\\ y/z\end{bmatrix} \tag{62}$$

We hereafter compute the necessary Lie derivatives of $\mathbf{h}$ and their gradients.

- *Zeroth-order Lie derivative* ($\mathfrak{L}^0\mathbf{h}$)

  $$\mathfrak{L}^0\mathbf{h} = \mathbf{h} = \begin{bmatrix} x/z\\ y/z\end{bmatrix}$$

  and its gradient is

  $$\nabla\mathfrak{L}^0\mathbf{h} = \begin{bmatrix}1/z & 0 & -x/z^2 & \mathbf{0}_{1\times 4}\\ 0 & 1/z & -y/z^2 & \mathbf{0}_{1\times 4}\end{bmatrix} \tag{63}$$

- *First-order Lie derivatives* ($\mathfrak{L}^1_{\mathbf{f}_1}\mathbf{h}$ and $\mathfrak{L}^1_{\mathbf{f}_2}\mathbf{h}$)

  $$\mathfrak{L}^1_{\mathbf{f}_1}\mathbf{h} = \nabla\mathfrak{L}^0\mathbf{h}\cdot\mathbf{f}_1 = \begin{bmatrix}-1/z & 0 & x/z^2\\ 0 & -1/z & y/z^2\end{bmatrix}$$

  Since $\mathfrak{L}^1_{\mathbf{f}_1}\mathbf{h}(1,1) = -1/z$, we have:

  $$\nabla\mathfrak{L}^1_{\mathbf{f}_1}\mathbf{h}(1,1) = \begin{bmatrix}\nabla_{\mathbf{p}}\mathfrak{L}^1_{\mathbf{f}_1}\mathbf{h}(1,1) & \mathbf{0}_{1\times 4}\end{bmatrix} \tag{64}$$

  with

  $$\nabla_{\mathbf{p}}\mathfrak{L}^1_{\mathbf{f}_1}\mathbf{h}(1,1) = \begin{bmatrix}0 & 0 & 1/z^2\end{bmatrix} \tag{65}$$

  Additionally,

  $$\mathfrak{L}^1_{\mathbf{f}_2}\mathbf{h} = \nabla\mathfrak{L}^0\mathbf{h}\cdot\mathbf{f}_2 = \begin{bmatrix}1/z & 0 & -x/z^2\\ 0 & 1/z & -y/z^2\end{bmatrix}\mathbf{C}$$

  Note that the dimension of $\mathfrak{L}^1_{\mathbf{f}_2}\mathbf{h}$ is 2×3. We stack the columns of $\mathfrak{L}^1_{\mathbf{f}_2}\mathbf{h}$ to form a 6×1 vector and its gradient (a 6×7 matrix) is:

  $$\nabla\mathfrak{L}^1_{\mathbf{f}_2}\mathbf{h} = \begin{bmatrix}\nabla_{\mathbf{p}}\mathfrak{L}^1_{\mathbf{f}_2}\mathbf{h} & \nabla_{\bar{q}}\mathfrak{L}^1_{\mathbf{f}_2}\mathbf{h}\end{bmatrix} \tag{66}$$

  where

  $$\nabla_{\bar{q}}\mathfrak{L}^1_{\mathbf{f}_2}\mathbf{h} = \frac{2}{z^2}\begin{bmatrix} zq_1-xq_3 & -zq_2-xq_4 & -zq_3-xq_1 & zq_4-xq_2\\ zq_2-yq_3 & zq_1-yq_4 & -zq_4-yq_1 & -zq_3-yq_2\\ zq_2+xq_4 & zq_1-xq_3 & zq_4-xq_2 & zq_3+xq_1\\ -zq_1+yq_4 & zq_2-yq_3 & -zq_3-yq_2 & zq_4+yq_1\\ zq_3+xq_1 & -zq_4+xq_2 & zq_1-xq_3 & -zq_2-xq_4\\ zq_4+yq_1 & zq_3+yq_2 & zq_2-yq_3 & zq_1-yq_4\end{bmatrix}$$

  Notice that we do not need the explicit form for $\nabla_{\mathbf{p}}\mathfrak{L}^1_{\mathbf{f}_2}\mathbf{h}$, since it will not affect the observability analysis.

Based on the above Lie derivatives and their gradients, we are ready to present the observability analysis of the system with robot R_1 equipped with a bearing-only sensor:

Lemma 2: Given bearing measurements, a sufficient condition for the system described by (56) and (62) to be locally weakly observable is (i) $\mathbf{v}_1 \neq \mathbf{0}$ and (ii) $\mathbf{v}_2 \neq \mathbf{0}$.

Proof: We stack the gradients of the Lie derivatives [see (63), (64), and (66)] to form the following observability matrix (of dimensions 9×7):

$$\mathcal{O}_2 = \left[\begin{array}{c:c}\nabla_{\mathbf{p}}\mathfrak{L}^0\mathbf{h} & \mathbf{0}_{2\times 4}\\ \nabla_{\mathbf{p}}\mathfrak{L}^1_{\mathbf{f}_1}\mathbf{h}(1,1) & \mathbf{0}_{1\times 4}\\ \hdashline \nabla_{\mathbf{p}}\mathfrak{L}^1_{\mathbf{f}_2}\mathbf{h} & \nabla_{\bar{q}}\mathfrak{L}^1_{\mathbf{f}_2}\mathbf{h}\end{array}\right] \tag{67}$$

In order to show that $\mathcal{O}_2$ is full (column) rank, it suffices to show that both $\begin{bmatrix} \nabla_{\mathbf{p}} \mathfrak{L}^0 \mathbf{h} \\ \nabla_{\mathbf{p}} \mathfrak{L}^1_{\mathbf{f}_1} \mathbf{h}(1,1) \end{bmatrix}$ and $\nabla_{\bar{q}} \mathfrak{L}^1_{\mathbf{f}_2} \mathbf{h}$ are full rank. The first matrix is upper triangular with determinant $1/z^4 \neq 0$ due to the physical constraint that the depth z is always strictly positive, i.e., the observed robot is in front of the camera.

To show that $\nabla_{\bar{q}} \mathfrak{L}^1_{\mathbf{f}_2} \mathbf{h}$ is full (column) rank, we proceed as follows:

$$\det\big((\nabla_{\bar{q}} \mathfrak{L}^1_{\mathbf{f}_2} \mathbf{h})^T (\nabla_{\bar{q}} \mathfrak{L}^1_{\mathbf{f}_2} \mathbf{h})\big) = \frac{4^4 (q_1^2+q_2^2+q_3^2+q_4^2)^4 (x^2+y^2+z^2)(x^2+y^2+2z^2)^2}{z^{14}} \neq 0$$

due to the fact that: (i) $q_1^2+q_2^2+q_3^2+q_4^2 = 1$, (ii) $x^2+y^2+z^2 > 0$, and (iii) $z > 0$. Thus $\nabla_{\bar{q}} \mathfrak{L}^1_{\mathbf{f}_2} \mathbf{h}$ is full rank.

Hence, we conclude that $\mathcal{O}_2$ is also full (column) rank, i.e., $\mathrm{rank}(\mathcal{O}_2) = 7$, therefore the system with one bearing-only sensor is locally weakly observable. ■

At this point we note that we have also examined the observability of the system with mutual bearing measurements (i.e., when both robots are equipped with bearing-only sensors). We have shown that the sufficient condition for the system using two bearing-only sensors to be locally weakly observable only requires robot R_1's movement ($\mathbf{v}_1 \neq \mathbf{0}$); this is a less restrictive condition compared to the single bearing sensor case, which requires motion of both robots (see Lemma 2). Due to space limitations, we will not include the detailed proof here but refer instead to [50].

3) Distance-only measurements: For clarity of presentation, the measurement function is chosen to be the square distance between the two robots divided by two, $d^2/2$, instead of the distance, d, i.e.,

$$h(\mathbf{x}) = \frac{d^2}{2} = \frac{1}{2}\mathbf{p}^T\mathbf{p} \tag{68}$$

Note that d and $d^2/2$ are both strictly positive, there is a one-to-one correspondence between them, and they provide the same information for the spatial relation of the two robots.

We hereafter compute the necessary Lie derivatives of h and their gradients.

- *Zeroth-order Lie derivative* ($\mathfrak{L}^0 h$)

  $$\mathfrak{L}^0 h = h = \frac{1}{2}\mathbf{p}^T\mathbf{p}$$

  and its gradient is

  $$\nabla \mathfrak{L}^0 h = \begin{bmatrix} \mathbf{p}^T & \mathbf{0}_{1\times 4} \end{bmatrix} \tag{69}$$

- *First-order Lie derivative* ($\mathfrak{L}^1_{\mathbf{f}_1} h$)

  $$\mathfrak{L}^1_{\mathbf{f}_1} h = \nabla \mathfrak{L}^0 h \cdot \mathbf{f}_1 = -\mathbf{p}^T$$

  and its gradient is

  $$\nabla \mathfrak{L}^1_{\mathbf{f}_1} h = \begin{bmatrix} -\mathbf{I}_3 & \mathbf{0}_{3\times 4} \end{bmatrix} \tag{70}$$

- *Second-order Lie derivative* ($\mathfrak{L}^2_{\mathbf{f}_2\mathbf{f}_1} h$)

  $$\mathfrak{L}^2_{\mathbf{f}_2\mathbf{f}_1} h = (\nabla \mathfrak{L}^1_{\mathbf{f}_1} h) \cdot \mathbf{f}_2 = \begin{bmatrix} -\mathbf{I}_3 & \mathbf{0}_{3\times 4} \end{bmatrix} \begin{bmatrix} \mathbf{C} \\ \mathbf{0}_{4\times 3} \end{bmatrix} = -\mathbf{C}$$

Similar Lie derivatives also appear in the case of distance and bearing measurements [see (59)] with only a sign difference. We have already shown that $\nabla_{\bar{q}}(\mathbf{C})$ has full column rank [see (60)]. Therefore, $\nabla_{\bar{q}}(-\mathbf{C})$ and equivalently $\nabla_{\bar{q}} \mathfrak{L}^2_{\mathbf{f}_2\mathbf{f}_1} h$ also has full column rank.

At this point, we are ready to present the main result of the observability of the system (56) with distance-only measurements (68):

Lemma 3: Given distance measurements, a sufficient condition for the system described by (56) and (68) to be locally weakly observable is (i) $\mathbf{v}_1 \neq \mathbf{0}$ and (ii) $\mathbf{v}_2 \neq \mathbf{0}$.

Proof: When conditions (i)-(ii) are satisfied, the observability matrix

$$\mathcal{O}_3 = \begin{bmatrix} \nabla \mathfrak{L}^1_{\mathbf{f}_1} h \\ \nabla \mathfrak{L}^2_{\mathbf{f}_2\mathbf{f}_1} h \end{bmatrix} \tag{71}$$

$$= \begin{bmatrix} -\mathbf{I}_3 & \mathbf{0}_{3\times 4} \\ \mathbf{0}_{9\times 3} & \nabla_{\bar{q}} \mathfrak{L}^2_{\mathbf{f}_2\mathbf{f}_1} h \end{bmatrix} \tag{72}$$

is full rank (note that we have already shown that $\nabla_{\bar{q}} \mathfrak{L}^2_{\mathbf{f}_2\mathbf{f}_1} h$ is full rank). From Theorem 1, the system is therefore locally weakly observable. ■

VIII. Weighted Least Squares Refinement

In the presence of noise, the analytical solutions developed in the previous sections are suboptimal, because they do not properly account for the uncertainty associated with each measurement. In most cases in practice, we are interested in the maximum likelihood estimate (MLE) of the relative pose. The MLE is determined by a nonlinear, iterative WLS algorithm, which needs an accurate initial estimate in order to quickly converge to the optimal solution. In our work, the WLS is initialized with the relative pose estimate provided by the analytic algorithms (see Sections IV, V, and VI).

In our formulation, we use the standard additive error model for position,[4]

$$\mathbf{p} = \hat{\mathbf{p}} + \tilde{\mathbf{p}} \tag{73}$$

but a multiplicative error model for the quaternion. In particular, true attitude, $\bar{q}$, estimated attitude, $\hat{\bar{q}}$, and error quaternion, $\delta\bar{q}$ are related via

$$\bar{q} = \delta\bar{q} \otimes \hat{\bar{q}} \tag{74}$$

Intuitively, $\delta\bar{q}$ describes the small rotation that makes the estimated and the true orientation coincide. Using the small-angle approximation, the error quaternion can be written as

$$\delta\bar{q} \simeq \begin{bmatrix} \frac{1}{2}\delta\boldsymbol{\theta}^T & 1 \end{bmatrix}^T \Leftrightarrow \mathbf{C} \simeq (\mathbf{I}_3 - \lfloor \delta\boldsymbol{\theta} \times \rfloor)\hat{\mathbf{C}} \tag{75}$$

The three-element parameterization $\delta\boldsymbol{\theta}$ is a minimal error representation and thus avoids the loss of rank of the covariance matrix, which would arise in the standard, additive, four-element parameterization due to the unit quaternion constraint. Following this error parameterization, the errors for the robot-to-robot relative translation, $\mathbf{p}_0$, and orientation, $\bar{q}_0$, will be denoted as $\tilde{\mathbf{p}}_0$ and $\delta\boldsymbol{\theta}_0$.

The error in the robot poses $\mathbf{r}_{1,k} = \begin{bmatrix} \bar{q}_{1,k}^T & \mathbf{p}_{1,k}^T \end{bmatrix}^T$ and $\mathbf{r}_{2,k} = \begin{bmatrix} \bar{q}_{2,k}^T & \mathbf{p}_{2,k}^T \end{bmatrix}^T$, arising from dead reckoning, e.g., by integration of linear and rotational velocity, will hence be

[4] We will denote estimated quantities by "$\hat{\ }$", and errors by "$\tilde{\ }$".

given by $\tilde{\mathbf{r}}_{1,k} = \begin{bmatrix}\delta\boldsymbol{\theta}_{1,k}^T & \tilde{\mathbf{p}}_{1,k}^T\end{bmatrix}^T$ and $\tilde{\mathbf{r}}_{2,k} = \begin{bmatrix}\delta\boldsymbol{\theta}_{2,k}^T & \tilde{\mathbf{p}}_{2,k}^T\end{bmatrix}^T$, and assumed to be zero mean Gaussian. In general, the dead reckoning errors for the same robot will be correlated, but those between two different robots will be independent. Notice that up to this point, the robots cannot perform cooperative localization [4] using the robot-to-robot measurements (which would create correlations between their estimates), because the relative pose between them is still unknown.

Assuming that the distance measurements are corrupted by white, zero-mean Gaussian noise, we write the measurement equation as

$$z_{d_k} = d_k + n_{d_k} \tag{76}$$

with the inter-robot distance, d_k, defined as the 2-norm of vector $\mathbf{p}_k$ [see (28)]. We only consider one distance measurement per time step. If two independent distance measurements from both robots are available, then these can be combined into a single distance measurement with appropriately reduced variance.

The bearing measurements are modeled as perspective projections for normalized, calibrated cameras

$$\mathbf{z}_{b_{1,k}} = \mathbf{b}_{1,k} + \mathbf{n}_{b_{1,k}} \tag{77}$$
$$\mathbf{z}_{b_{2,k}} = \mathbf{b}_{2,k} + \mathbf{n}_{b_{2,k}} \tag{78}$$

All measurements can be stacked to form the augmented measurement vector $\mathbf{z}_k = \begin{bmatrix}z_{d_k} & \mathbf{z}_{b_{1,k}}^T & \mathbf{z}_{b_{2,k}}^T\end{bmatrix}^T$. To recall, the measured quantities are given in terms of the robot local relative poses as [see (29), (62), and (10)]

$$\begin{aligned}
\mathbf{p}_k &= \mathbf{C}_{1,k}(\mathbf{p}_0 + \mathbf{C}_0\,\mathbf{p}_{2,k} - \mathbf{p}_{1,k}) \\
d_k &= \sqrt{\mathbf{p}_k^T\mathbf{p}_k} \\
\mathbf{b}_{1,k} &= \Pi\frac{\mathbf{p}_k}{\begin{bmatrix}0 & 0 & 1\end{bmatrix}\mathbf{p}_k} \\
\mathbf{b}_{2,k} &= \Pi\frac{\mathbf{C}_{2,k}\,\mathbf{C}_0^T\,\mathbf{C}_{1,k}^T\,\mathbf{p}_k}{\begin{bmatrix}0 & 0 & 1\end{bmatrix}\mathbf{C}_{2,k}\,\mathbf{C}_0^T\,\mathbf{C}_{1,k}^T\,\mathbf{p}_k}
\end{aligned}$$

where $\Pi = \begin{bmatrix}\mathbf{I}_2 & \mathbf{0}_{2\times 1}\end{bmatrix}$ denotes the projection matrix.

We linearize the measurement equations around the current estimate of the robot-to-robot pose, as well as the individual robot poses, which we treat as nuisance parameters. Using the chain rule, we compute the Jacobians as

$$\mathbf{H}_{\theta_{0,k}} = \frac{\partial\mathbf{z}_k}{\partial\boldsymbol{\theta}_0} = \begin{bmatrix}\mathbf{p}_k^T\mathbf{C}_{1,k}\lfloor\mathbf{C}_0\mathbf{p}_{2,k}\times\rfloor/d_k \\ \mathbf{H}_{b_{1,k}}\mathbf{C}_{1,k}\lfloor\mathbf{C}_0\mathbf{p}_{2,k}\times\rfloor \\ \mathbf{H}_{b_{2,k}}\mathbf{C}_{2,k}\mathbf{C}_0^T\lfloor\mathbf{p}_{1,k} - \mathbf{p}_0\times\rfloor\end{bmatrix}$$

$$\mathbf{H}_{p_{0,k}} = \frac{\partial\mathbf{z}_k}{\partial\mathbf{p}_0} = \begin{bmatrix}\mathbf{p}_k^T\mathbf{C}_{1,k}/d_k \\ \mathbf{H}_{b_{1,k}}\mathbf{C}_{1,k} \\ \mathbf{H}_{b_{2,k}}\mathbf{C}_{2,k}\mathbf{C}_0^T\end{bmatrix}$$

$$\mathbf{H}_{R_{1,k}} = \frac{\partial\mathbf{z}_k}{\partial\mathbf{r}_{1,k}} = \begin{bmatrix}\begin{bmatrix}\mathbf{0}_{1\times 3} & -\mathbf{p}_k^T\mathbf{C}_{1,k}/d_k\end{bmatrix} \\ \mathbf{H}_{b_{1,k}}\begin{bmatrix}\lfloor\mathbf{p}_k\times\rfloor & -\mathbf{C}_{1,k}\end{bmatrix} \\ \mathbf{H}_{b_{2,k}}\begin{bmatrix}\mathbf{0}_{3\times 3} & -\mathbf{C}_{2,k}\mathbf{C}_0^T\end{bmatrix}\end{bmatrix}$$

$$\mathbf{H}_{R_{2,k}} = \frac{\partial\mathbf{z}_k}{\partial\mathbf{r}_{2,k}} = \begin{bmatrix}\begin{bmatrix}\mathbf{0}_{1\times 3} & \mathbf{p}_k^T\mathbf{C}_{1,k}\mathbf{C}_0/d_k\end{bmatrix} \\ \mathbf{H}_{b_{1,k}}\begin{bmatrix}\mathbf{0}_{3\times 3} & \mathbf{C}_{1,k}\mathbf{C}_0\end{bmatrix} \\ \mathbf{H}_{b_{2,k}}\begin{bmatrix}\lfloor\mathbf{C}_{2,k}\,\mathbf{C}_0^T\,\mathbf{C}_{1,k}^T\,\mathbf{p}_k\times\rfloor & \mathbf{C}_{2,k}\end{bmatrix}\end{bmatrix}$$

where

$$\mathbf{H}_{b_{1,k}} = \frac{1}{\begin{bmatrix}0 & 0 & 1\end{bmatrix}\mathbf{p}_k}\begin{bmatrix}\mathbf{I}_2 & -\mathbf{b}_{1,k}\end{bmatrix}$$

$$\mathbf{H}_{b_{2,k}} = \frac{1}{\begin{bmatrix}0 & 0 & 1\end{bmatrix}(\mathbf{C}_{2,k}\,\mathbf{C}_0^T\,\mathbf{C}_{1,k}^T\,\mathbf{p}_k)}\begin{bmatrix}\mathbf{I}_2 & -\mathbf{b}_{2,k}\end{bmatrix}$$

and evaluate them at the current linearization point.

The measurement residual at time-step k can now be approximated as

$$\begin{aligned}
\tilde{\mathbf{z}}_k &= \mathbf{z}_k - \hat{\mathbf{z}}_k \\
&\simeq \begin{bmatrix}\mathbf{H}_{\theta_{0,k}} & \mathbf{H}_{p_{0,k}}\end{bmatrix}\begin{bmatrix}\delta\boldsymbol{\theta}_0 \\ \tilde{\mathbf{p}}_0\end{bmatrix} + \mathbf{H}_{R_{1,k}}\tilde{\mathbf{r}}_{1,k} + \mathbf{H}_{R_{2,k}}\tilde{\mathbf{r}}_{2,k} + \mathbf{n}_k
\end{aligned}$$

where $\mathbf{n}_k = \begin{bmatrix}n_{d_k} & \mathbf{n}_{b_{1,k}}^T & \mathbf{n}_{b_{2,k}}^T\end{bmatrix}^T$ [see (76), (77), and (78)] is white, zero-mean Gaussian noise with covariance $\mathbf{R}_k$.

Stacking all available measurements yields the linearized measurement error equation

$$\tilde{\mathbf{z}} \simeq \mathbf{H}\begin{bmatrix}\delta\boldsymbol{\theta}_0 \\ \tilde{\mathbf{p}}_0\end{bmatrix} + \mathbf{H}_{R_1}\tilde{\mathbf{r}}_1 + \mathbf{H}_{R_2}\tilde{\mathbf{r}}_2 + \mathbf{n}$$

where $\mathbf{H} = \begin{bmatrix}\mathbf{H}_{\theta_0} & \mathbf{H}_{p_0}\end{bmatrix}$, $\mathbf{H}_{\theta_0}$ and $\mathbf{H}_{p_0}$ contain the stacked Jacobians $\mathbf{H}_{\theta_{0,k}}$ and $\mathbf{H}_{p_{0,k}}$, $\tilde{\mathbf{r}}_1$ and $\tilde{\mathbf{r}}_2$ contain the stacked robot pose error vectors, and $\mathbf{H}_{R_1}$, $\mathbf{H}_{R_2}$ are block diagonal matrices with the Jacobians $\mathbf{H}_{R_{1,k}}$ and $\mathbf{H}_{R_{2,k}}$ at the appropriate row/column positions.

Assuming Gaussian measurement noise $\mathbf{n}$ with covariance $\mathbf{R}$, and Gaussian noise in the robot pose estimates $\hat{\mathbf{r}}_1$ and $\hat{\mathbf{r}}_2$ with covariances $\mathbf{P}_{R_1}$ and $\mathbf{P}_{R_2}$, we can write the residual covariance (the weighting matrix) as

$$\mathbf{W} = \mathbf{H}_{R_1}\mathbf{P}_{R_1}\mathbf{H}_{R_1}^T + \mathbf{H}_{R_2}\mathbf{P}_{R_2}\mathbf{H}_{R_2}^T + \mathbf{R}$$

We find the correction by solving the weighted normal equations [51]:

$$\mathbf{H}^T\mathbf{W}^{-1}\mathbf{H}\begin{bmatrix}\delta\boldsymbol{\theta}_0 \\ \tilde{\mathbf{p}}_0\end{bmatrix} = \mathbf{H}^T\mathbf{W}^{-1}(\mathbf{z} - \hat{\mathbf{z}})$$

Note that a prerequisite for computing the correction, as well as the covariance matrix, is for the measurement matrix $\mathbf{H}$ to be of full column rank[5].

At each iteration of the WLS algorithm, we update the robot-to-robot position and quaternion as

$$\begin{aligned}
\hat{\mathbf{p}}_0^{j+1} &= \hat{\mathbf{p}}_0^j + \tilde{\mathbf{p}}_0 \\
\hat{\bar{q}}_0^{j+1} &= \delta\bar{q}_0 \otimes \hat{\bar{q}}_0^j, \quad \delta\bar{q}_0 = \frac{\begin{bmatrix}\frac{1}{2}\delta\boldsymbol{\theta}_0^T & 1\end{bmatrix}^T}{||\begin{bmatrix}\frac{1}{2}\delta\boldsymbol{\theta}_0^T & 1\end{bmatrix}||}
\end{aligned} \tag{79}$$

This process is repeated to convergence, using the latest estimates, $\hat{\mathbf{p}}_0^{j+1}$ and $\hat{\bar{q}}_0^{j+1}$, as linearization points when computing $\mathbf{H}$ and $\mathbf{W}$.

The final covariance of the estimate is given by

$$E\left[\begin{bmatrix}\delta\boldsymbol{\theta}_0 \\ \tilde{\mathbf{p}}_0\end{bmatrix}\begin{bmatrix}\delta\boldsymbol{\theta}_0 \\ \tilde{\mathbf{p}}_0\end{bmatrix}^T\right] = \left(\mathbf{H}^T\mathbf{W}^{-1}\mathbf{H}\right)^{-1} \tag{80}$$

[5]Full rank of $\mathbf{H}$ is ensured generically (i.e., for randomly selected control inputs) if the system is locally weakly observable, a sufficient number of measurements have been collected, and the linearization point is sufficiently close to a local optimum.

Once a pose estimate and its covariance are computed, additional distance or bearing measurements can be processed in a recursive estimator, such as an extended Kalman filter [4].

IX. Simulation Results

We have evaluated the performance of our algorithms in simulations, for different values of noise covariance in egomotion and robot-to-robot measurements. In particular, random trajectories were generated with the two robots being on average 1 m - 2 m apart, and moving an average of 3 m - 6 m between each of a total of 10 distance and/or bearing measurements per simulation.

Egomotion was determined by integrating noisy measurements of turn rate, $\boldsymbol{\omega}$, and velocity, $\mathbf{v}$, in the body frame. This corresponds to a simplified model of inertial navigation. The continuous-time ground-truth motion model for the i-th robot is given by

$$\dot{\mathbf{p}}_i = \mathbf{C}_i^T \mathbf{v}_i \tag{81}$$

$$\dot{\bar{q}}_i = \frac{1}{2} \begin{bmatrix} -\lfloor \boldsymbol{\omega}_i \times \rfloor & \boldsymbol{\omega}_i \\ -\boldsymbol{\omega}_i^{\mathrm{T}} & 0 \end{bmatrix} \bar{q}_i \tag{82}$$

For dead-reckoning, the linear and rotational velocities in (81) and (82) have to be replaced by noisy measurements. These measurements are assumed to be corrupted by zero-mean, Gaussian noise with covariance $\mathbf{Q}_i = \mathrm{blkdiag}(\sigma_\omega^2 \cdot \mathbf{I}_3,\ \sigma_v^2 \cdot \mathbf{I}_3)$, i.e.,

$$\boldsymbol{\omega}_{m,i} = \boldsymbol{\omega}_i + \mathbf{n}_{\omega_i} \tag{83}$$

$$\mathbf{v}_{m,i} = \mathbf{v}_i + \mathbf{n}_{v_i} \tag{84}$$

The corresponding continuous-time error model is given by [36]:

$$\begin{bmatrix} \dot{\delta\boldsymbol{\theta}}_i \\ \dot{\tilde{\mathbf{p}}}_i \end{bmatrix} = \mathbf{F}_i \begin{bmatrix} \delta\boldsymbol{\theta}_i \\ \tilde{\mathbf{p}}_i \end{bmatrix} + \mathbf{G}_i \begin{bmatrix} \mathbf{n}_{\omega_i} \\ \mathbf{n}_{v_i} \end{bmatrix} \tag{85}$$

$$\mathbf{F}_i = \begin{bmatrix} -\lfloor \boldsymbol{\omega}_{m,i} \times \rfloor & \mathbf{0}_{3\times 3} \\ -\hat{\mathbf{C}}_i^T \lfloor \mathbf{v}_{m,i} \times \rfloor & \mathbf{0}_{3\times 3} \end{bmatrix}, \quad \mathbf{G}_i = \begin{bmatrix} -\mathbf{I}_3 & \mathbf{0}_{3\times 3} \\ \mathbf{0}_{3\times 3} & -\hat{\mathbf{C}}_i^T \end{bmatrix}$$

At any time, the current pose and corresponding covariance matrix can be computed by numerical integration of the system model, (81)-(82), and the continuous-time Lyapunov equation

$$\dot{\mathbf{P}}_i = \mathbf{F}_i \mathbf{P}_i + \mathbf{P}_i \mathbf{F}_i^T + \mathbf{G}_i \mathbf{Q}_i \mathbf{G}_i^T \tag{86}$$

At each point where a robot-to-robot measurement is registered, the state vector is augmented by a static copy of the current pose and covariance matrix to correctly account for the correlations. Since each robot navigates using dead-reckoning and does *not* perform cooperative localization, we note that the pose estimates of the two robots are independent.

The noise in the robot-to-robot distance and bearing measurements [see (76)-(78)] is assumed zero-mean white Gaussian with covariance $\mathbf{R}_k = \mathrm{blkdiag}(\sigma_d^2, \sigma_b^2 \cdot \mathbf{I}_4)$.

We have conducted Monte Carlo simulations for different settings of the noise covariances, and report the averaged results of 1000 simulations per setting. To keep the number of independent parameters reasonable, we have set $\sigma_v = 10\,\mathrm{m} \cdot \sigma_\omega$ and $\sigma_d = 10\,\mathrm{m} \cdot \sigma_b$.

Figs. 3-5 show the results for range and bearing, bearing-only, and distance-only measurements. In particular, Figs. 3(a)-5(a) show the error in relative position produced by the closed-form algorithms, as a function of the measurement and odometry noise standard deviations. In all cases, we can see that the closed-form solution yields convincing results, in particular for low noise variance [see Figs. 3(b)-5(b)], at high speed and negligible computational cost. Note, however, that in all but the cases of negligible noise, a WLS refinement step is advisable to produce accurate estimates, since the algebraic method is exact only in the noise-free case.

Figs. 3(b)-5(b), 3(c)-5(c), and 3(d)-5(d) compare the position error, the attitude error, and the measurement residual of the algebraic method against those obtained through WLS, once using the algebraic method's result for initialization, and once with a random initial guess. Note that any iterative method, such as WLS, requires an initial estimate whose accuracy greatly impacts the speed of convergence and quality of the solution. Poor initial estimates can result in local minima and even divergence.

This finding is corroborated by the number of iterations required for convergence (using a threshold on the norm of the correction as stopping criterion). Figs. 3(e)-5(e) show that using the algebraic result for initialization requires roughly one third the number of iterations than that of the random initial guess. Furthermore, a random initial guess leads more often to divergence [see Figs. 3(f)-5(f)]. A particular instance of WLS refinement is considered as diverged, if it required more than 100 iterations, or if the Hessian became excessively ill-conditioned ($\kappa > 10^{10}$, where κ is the condition number of the Hessian). We attribute the large percentage of diverged cases for randomly initialized range and bearing or bearing only cases to a cost function with very narrow attractor basins for the minima. It is likely that a more efficient step-size control mechanism or regularization of the Hessian (e.g., using Levenberg-Marquardt) would improve the convergence behavior compared to the Gauss-Newton optimization scheme applied here, at the cost of increased computations. However, Gauss-Newton worked reasonably well when initialized using the closed-form expressions developed in Sections IV-VI.

X. Conclusion and Future Work

We have presented three algorithms for computing in closed form the 3D robot-to-robot relative pose, given known egomotion of two robots in their respective frames of reference, and robot-to-robot (i) range and bearing, (ii) bearing-only, and (iii) range-only measurements, respectively. In particular, the derived expressions are exact in the absence of noise and yield high-accuracy initial estimates for subsequent iterative WLS-refinement in the presence of noise. Additionally, we have provided a nonlinear observability study based on Lie derivatives, proving weak local observability for all three cases of different robot-to-robot measurements mentioned above.

This work opens several paths for future research. One example is the study of the 3D robot-to-robot pose problem when a mixture of sensors are available, or a heterogeneous team of robots is deployed (e.g., one robot is equipped with

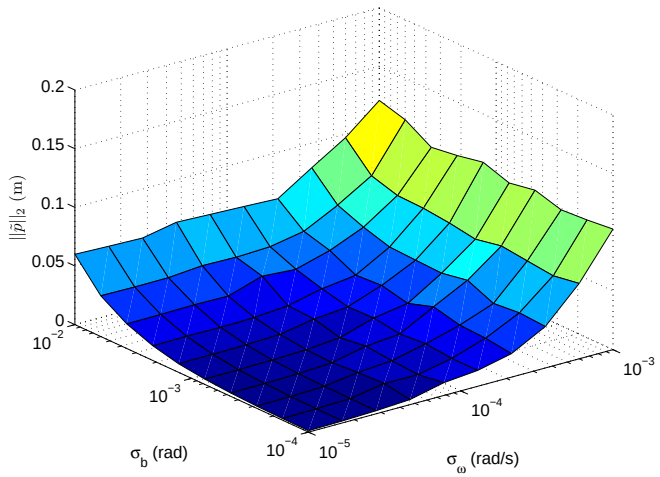

(a) Norm of position error. Range- and bearing measurement noise standard deviations were set to $\sigma_d = 10\,\mathrm{m} \cdot \sigma_b$.

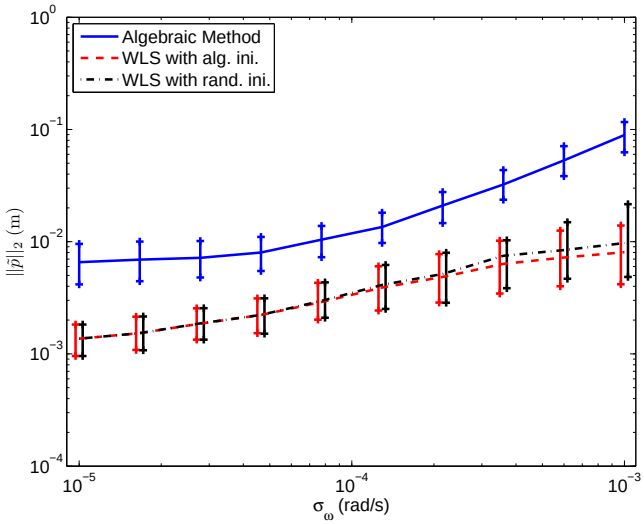

(b) Norm of position error.

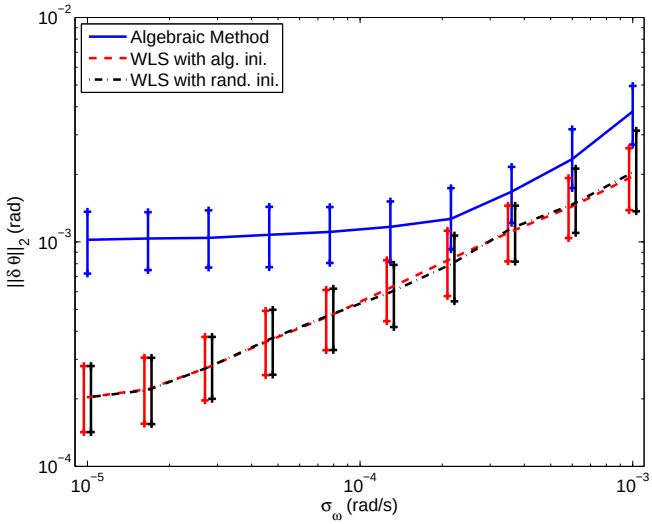

(c) Norm of attitude error.

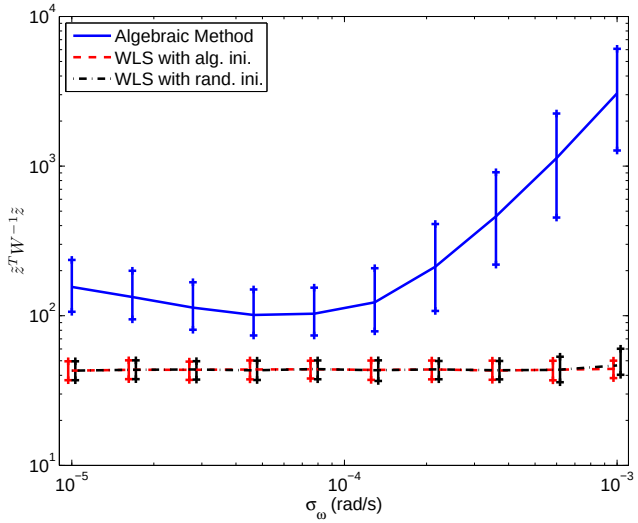

(d) Norm of weighted measurement residual.

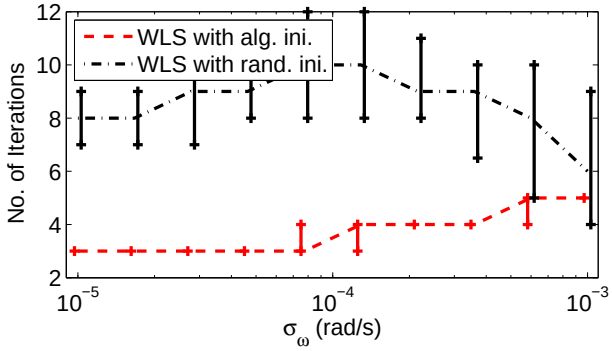

(e) Median number of iterations needed for convergence.

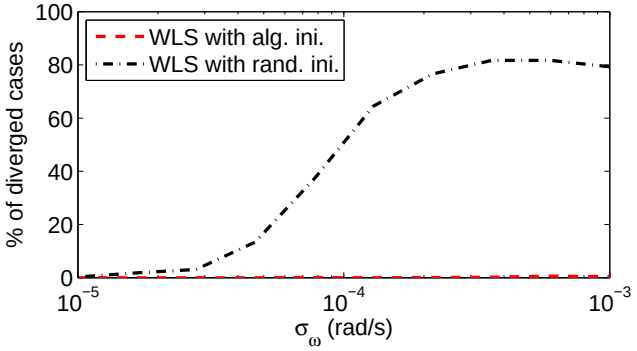

(f) Percentage of divergence in WLS.

Fig. 3. Simulation results for the algebraic method and WLS refinement (using as initial estimate the result from the algebraic method or a random initialization) for the case of *range and bearing* measurements. Shown is the dependence on system and measurement noise standard deviations. The results for each setting were averaged over 1000 trials. The inter-robot distances were between 1 m-2 m, and the robots moved 3 m-6 m between measurements. Plots 3(b)-3(f) show results (median and 25-75% quartiles) for a fixed bearing measurement noise of $3\sigma_b = 0.0039$ rad and range noise of $3\sigma_d = 3.9$ cm, as function of the egomotion noise standard deviation σ_ω. The linear velocity noise standard deviation was set to $\sigma_v = 10\,\mathrm{m} \cdot \sigma_\omega$. Notice that the randomly initialized WLS requires significantly more iterations to converge, and diverges easily if poorly initialized, especially for larger noise values. The residuals are computed only for the converged cases, which explains the similar accuracy achieved by both WLS methods.

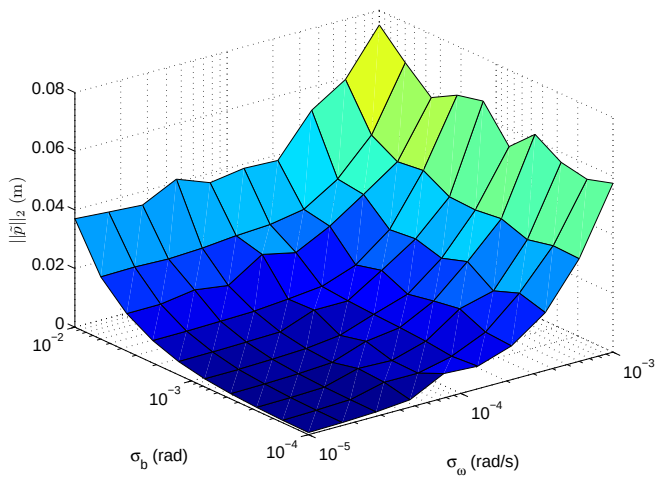

(a) Norm of position error

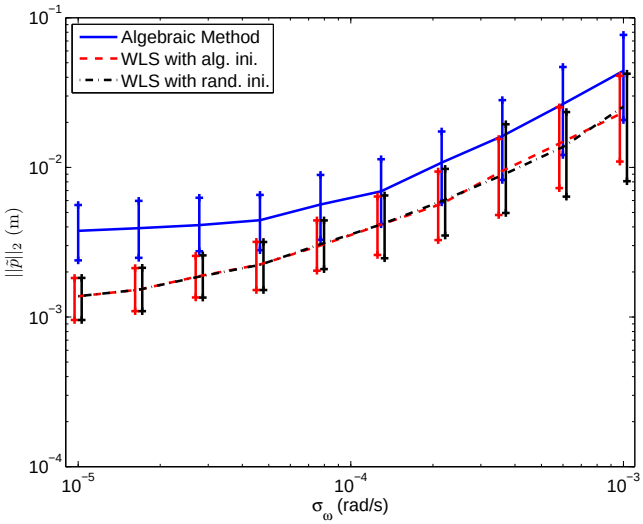

(b) Norm of position error.

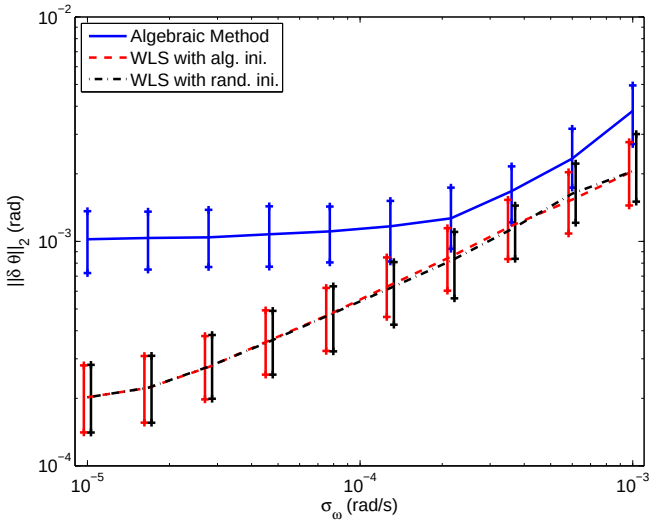

(c) Norm of attitude error.

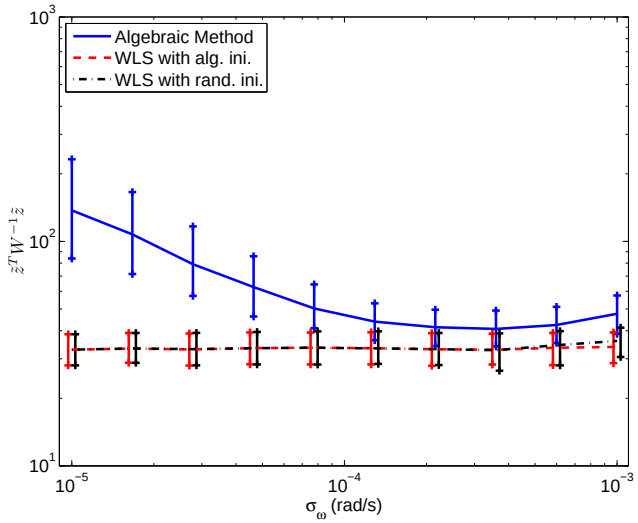

(d) Norm of weighted measurement residual.

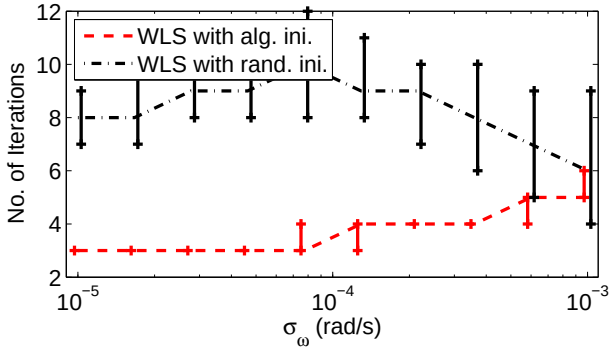

(e) Median number of iterations needed for convergence.

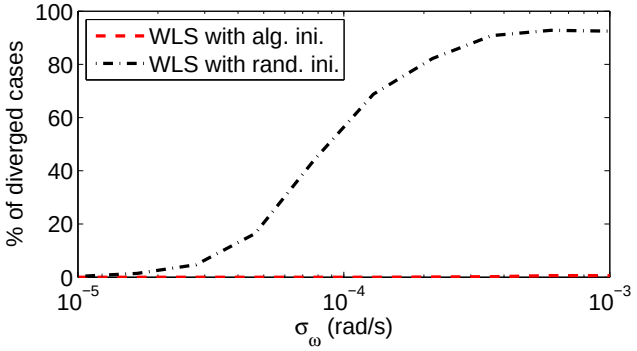

(f) Percentage of divergence in WLS.

Fig. 4. Simulation results for the algebraic method and WLS refinement (using as initial estimate the result from the algebraic method or a random initialization) for the case of *bearing-only* measurements. Shown is the dependence on system and measurement noise standard deviations. The results for each setting were averaged over 1000 trials. The inter-robot distances were between 1 m-2 m, and the robots moved 3 m-6 m between measurements. Plots 4(b)-4(f) show results (median and 25-75% quartiles) for a fixed bearing measurement noise of $3\sigma_b = 0.0039$ rad, as function of the egomotion noise standard deviation σ_ω. The linear velocity noise standard deviation was set to $\sigma_v = 10\,\mathrm{m} \cdot \sigma_\omega$. Notice that the randomly initialized WLS requires significantly more iterations to converge, and diverges easily if poorly initialized, especially for larger noise values. The residuals are computed only for the converged cases, which explains the similar accuracy achieved by both WLS methods.

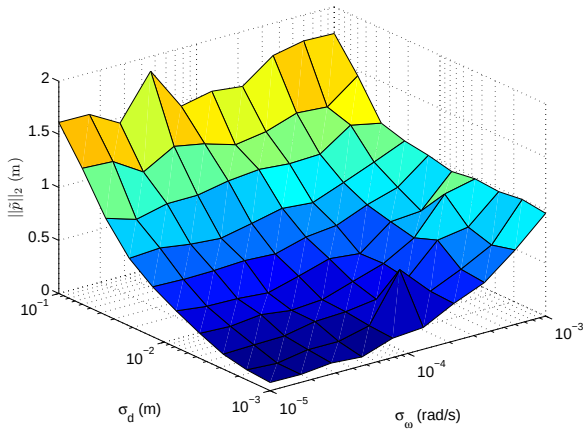

(a) Norm of position error

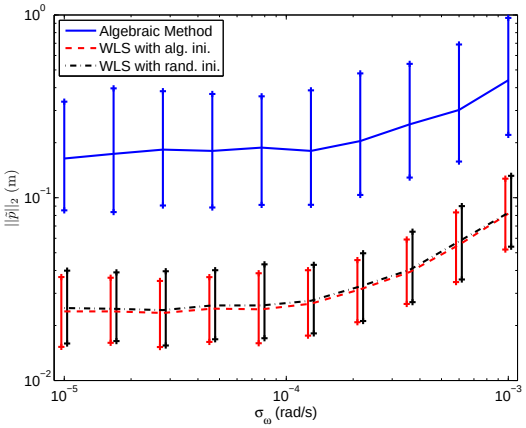

(b) Norm of position error.

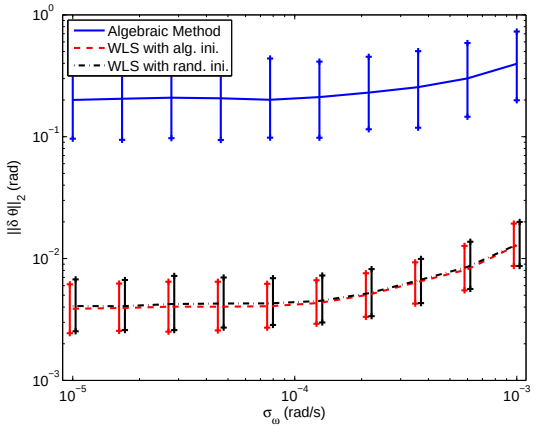

(c) Norm of attitude error.

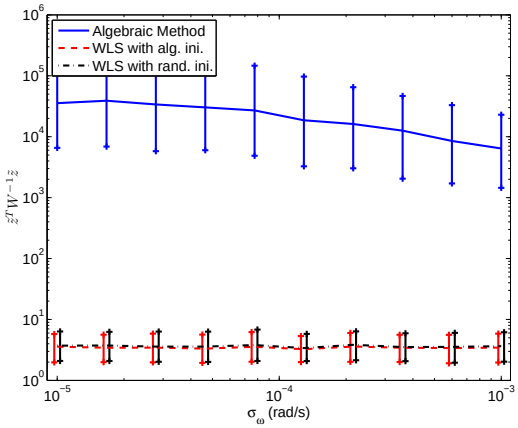

(d) Norm of weighted measurement residual.

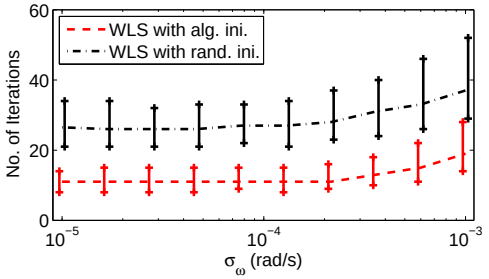

(e) Median number of iterations needed for convergence.

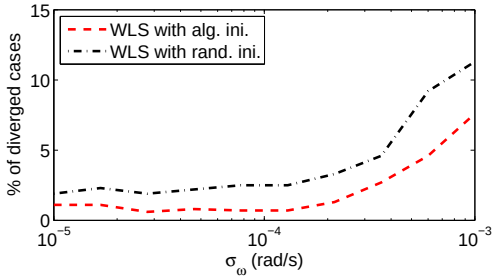

(f) Percentage of divergence in WLS.

Fig. 5. Simulation results for the algebraic method and WLS refinement (using as initial estimate the result from the algebraic method or a random initialization) for the case of *range-only* measurements. Shown is the dependence on system and measurement noise standard deviations. The results for each setting were averaged over 1000 trials. Plots 5(b)-5(f) show results (median and 25-75% quartiles) for a fixed measurement noise of $3\sigma_d = 3.9$ cm, as function of the egomotion noise standard deviation σ_ω. The linear velocity noise standard deviation was set to $\sigma_v = 10\,\mathrm{m} \cdot \sigma_\omega$.

a laser scanner that can measure range and bearing, but the other only has a camera that provides bearing). Further, we plan to investigate the inclusion of other sources of information. For instance, it is very common that a robot team shares certain information about the environment, such as measurements of the gravity vector, or of common targets (e.g., using star trackers). Moreover, we will consider including relative velocity measurements, which could be obtained from doppler radar [52]. A framework that allows inclusion of such additional information, and its impact on accuracy and ease of relative pose computation is the subject of ongoing work. Finally, based on our observability study, we are currently investigating optimal motion strategies for both robots in order to minimize the uncertainty of the relative pose.

APPENDIX

Quadratic Constraints in q_{ij}

Define the Veronese mapping $q_{ij} = q_i q_j, i, j = 1, \ldots, 4, j \geq i$. The 10 new variables q_{ij} are not independent, but are constrained to the Veronese variety defined by the

following 20 quadratic constraints:

$$\begin{array}{lll} q_{11}q_{44} = q_{14}^2 & q_{14}q_{24} = q_{12}q_{44} & q_{23}q_{34} = q_{33}q_{24} \\ q_{22}q_{44} = q_{24}^2 & q_{24}q_{34} = q_{23}q_{44} & q_{13}q_{34} = q_{33}q_{14} \\ q_{33}q_{44} = q_{34}^2 & q_{34}q_{14} = q_{13}q_{44} & q_{23}q_{24} = q_{22}q_{34} \\ q_{11}q_{22} = q_{12}^2 & q_{12}q_{13} = q_{11}q_{23} & q_{12}q_{24} = q_{22}q_{14} \\ q_{22}q_{33} = q_{23}^2 & q_{12}q_{23} = q_{22}q_{13} & q_{13}q_{14} = q_{11}q_{34} \\ q_{33}q_{11} = q_{13}^2 & q_{13}q_{23} = q_{33}q_{12} & q_{12}q_{14} = q_{11}q_{24} \\ & q_{12}q_{34} = q_{13}q_{24} & q_{12}q_{34} = q_{14}q_{23} \end{array}$$

These 20 constraints are exactly the consequence of the Veronese mapping. Specifically, by defining the ideal I generated by the 10 polynomials $q_{ij} - q_i q_j \in \mathbb{C}[q_1, \ldots, q_4, q_{11}, \ldots, q_{44}]$, $i, j = 1, \ldots, 4$, $j \geq i$, we find that the 20 constraints generate the elimination ideal $I \cap \mathbb{C}[q_{11}, \ldots, q_{44}]$ (e.g., by computing a Gröbner basis with respect to lex ordering). Moreover, by [43, Thm. 12, Ch. 8, Sec. 5], the variety defined by this elimination ideal is exactly equal to the image of the Veronese mapping.

ACKNOWLEDGEMENTS

This work was supported by the University of Minnesota (DTC), and the National Science Foundation (IIS-0643680, IIS-0811946, IIS-0835637).

REFERENCES

[1] A. Howard, M. Mataric, and G. Sukhatme, "Putting the 'I' in 'team': an ego-centric approach to cooperative localization," in *Proc. of the IEEE Int. Conf. on Robotics and Automation*, Taipei, Taiwan, Sep. 14–19 2003, pp. 868–874.

[2] R. Kurazume and S. Hirose, "An experimental study of a cooperative positioning system," *Autonomous Robots*, vol. 8, no. 1, pp. 43–52, Jan. 2000.

[3] I. Rekleitis, G. Dudek, and E. Milios, "Probabilistic cooperative localization and mapping in practice," in *Proc. of the IEEE Int. Conf. on Robotics and Automation*, Taipei, Taiwan, Sep. 14–19 2003, pp. 1907–1912.

[4] S. I. Roumeliotis and G. A. Bekey, "Distributed multirobot localization," *IEEE Trans. on Robotics and Automation*, vol. 18, no. 5, pp. 781–795, Oct. 2002.

[5] A. I. Mourikis and S. I. Roumeliotis, "Optimal sensor scheduling for resource constrained localization of mobile robot formations," *IEEE Trans. on Robotics*, vol. 22, no. 5, pp. 917–931, Oct. 2006.

[6] J. Fenwick, P. Newman, and J. Leonard, "Cooperative concurrent mapping and localization," in *Proc. of the IEEE Int. Conf. on Robotics and Automation*, Washington, D.C., May 11–15 2002, pp. 1810–1817.

[7] A. Howard, L. E. Parker, and G. S. Sukhatme, "Experiments with a large heterogeneous mobile robot team: Exploration, mapping, deployment and detection," *International Journal of Robotics Research*, vol. 25, no. 5-6, pp. 431–447, Sep. 2006.

[8] R. Madhavan, K. Fregene, and L. E. Parker, "Distributed cooperative outdoor multirobot localization and mapping," *Autonomous Robots, Special Issue on Analysis and Experiments in Distributed Multi-Robot Systems*, vol. 17, no. 1, pp. 23–39, Jul. 2004.

[9] M. D. Marco, A. Garulli, A. Giannitrapani, and A. Vicino, "Simultaneous localization and map building for a team of cooperating robots: a set membership approach," *IEEE Trans. on Robotics and Automation*, vol. 19, no. 2, pp. 238–249, Apr. 2003.

[10] S. Thrun, "A probabilistic online mapping algorithm for teams of mobile robots," *International Journal of Robotics Research*, vol. 20, no. 5, pp. 335–363, May 2001.

[11] B. Jung and G. S. Sukhatme, "Tracking targets using multiple robots: The effect of environment occlusion," *Autonomous Robots*, vol. 13, no. 3, pp. 191–205, Nov. 2002.

[12] M. Mazo, A. Speranzon, K. Johansson, and X. Hu, "Multi-robot tracking of a moving object using directional sensors," in *Proc. of the IEEE Int. Conf. on Robotics and Automation*, New Orleans, LA, Apr. 26–May 1 2004, pp. 1103–1108.

[13] L. E. Parker, "Distributed algorithms for multi-robot observation of multiple moving targets," *Autonomous Robots*, vol. 12, no. 3, pp. 231–255, May 2002.

[14] A. W. Stroupe, "Collaborative execution of exploration and tracking using move value estimation for robot teams (MVERT)," Ph.D. dissertation, Carnegie Mellon University, Sep. 2003.

[15] K. Zhou and S. I. Roumeliotis, "Optimal motion strategies for range-only constrained multi-sensor target tracking," *IEEE Trans. on Robotics*, vol. 24, no. 5, pp. 1168–1185, Oct. 2008.

[16] X. S. Zhou and S. I. Roumeliotis, "Multi-robot SLAM with unknown initial correspondence: The robot rendezvous case," in *Proc. of the IEEE/RSJ Int. Conf. on Intelligent Robots and Systems*, Beijing, China, Oct. 9–15 2006, pp. 1785–1792.

[17] ——, "Robot-to-robot relative pose estimation from range measurements," *IEEE Trans. on Robotics*, vol. 24, no. 6, pp. 1379–1393, Dec. 2008.

[18] N. Trawny, X. S. Zhou, K. X. Zhou, and S. I. Roumeliotis, "3D relative pose estimation from distance-only measurements," in *Proc. of the IEEE/RSJ Int. Conf. on Intelligent Robots and Systems*, San Diego, CA, Oct. 29–Nov. 2 2007, pp. 1071–1078.

[19] N. Trawny, X. S. Zhou, and S. I. Roumeliotis, "3D relative pose estimation from 6 distances," in *Proc. of Robotics: Science and Systems*, Seattle, WA, Jun. 28–Jul. 1 2009.

[20] J. Aspnes, T. Eren, D. K. Goldenberg, A. S. Morse, W. Whiteley, Y. R. Yang, B. D. O. Anderson, and P. N. Belhumeur, "A theory of network localization," *IEEE Trans. on Mobile Computing*, vol. 5, no. 12, pp. 1663–1678, Dec. 2006.

[21] L. Doherty, K. S. J. Pister, and L. E. Ghaoui, "Convex position estimation in wireless sensor networks," in *IEEE INFOCOM 2001. Proc. of the Twentieth Annual Joint Conf. of the IEEE Computer and Communications Societies*, Anchorage, AK, Apr. 22–26 2001, pp. 1655–1663.

[22] J. A. Costa, N. Patwari, and A. O. Hero III, "Distributed weighted-multidimensional scaling for node localization in sensor networks," *ACM Trans. on Sensor Networks*, vol. 2, no. 1, pp. 39–64, Feb. 2006.

[23] Y. Shang, W. Ruml, Y. Zhang, and M. P. J. Fromherz, "Localization from mere connectivity," in *Proc. of the 4th ACM Int. Symposium on Mobile Ad Hoc Networking and Computing*, Annapolis, MD, Jun. 1–3 2003, pp. 201–212.

[24] C.-H. Ou and K.-F. Ssu, "Sensor position determination with flying anchors in three-dimensional wireless sensor networks," *IEEE Trans. on Mobile Computing*, vol. 7, no. 9, pp. 1084–1097, Sep. 2008.

[25] S. Higo, T. Yoshimitsu, and I. Nakatani, "Localization on small body surface by radio ranging," in *Proc. of the 16th AAS/AIAA Space Flight Mechanics Conf.*, Tampa, FL, Jan. 22–26 2006.

[26] Y. Dieudonne, O. Labbani-Igbida, and F. Petit, "On the solvability of the localization problem in robot networks," in *Proc. of the IEEE Int. Conf. on Robotics and Automation*, Pasadena, CA, May 19–23 2008, pp. 480–485.

[27] A. Martinelli and R. Siegwart, "Observability analysis for mobile robot localization," in *Proc. of the IEEE/RSJ Int. Conf. on Intelligent Robots and Systems*, Edmonton, Canada, Aug. 2–6 2005, pp. 1471–1476.

[28] F. Beutler and U. D. Hanebeck, "Closed-form range-based posture estimation based on decoupling translation and orientation," in *Proc. of the IEEE Int. Conf. on Acoustics, Speech, and Signal Processing*, Philadelphia, PA, Mar. 18–23 2005, pp. 989–992.

[29] Z. Zhang, "A flexible new technique for camera calibration," *IEEE Trans. on Pattern Analysis and Machine Intelligence*, vol. 22, no. 11, pp. 1330–1334, Nov. 2000.

[30] I. Rekleitis, D. Meger, and G. Dudek, "Simultaneous planning, localization, and mapping in a camera sensor network," *Robotics and Autonomous Systems*, vol. 54, no. 11, pp. 921–932, Nov. 2006.

[31] D. Stewart, "A platform with six degrees of freedom," in *Proc. of the Institution of Mechanical Engineers*, vol. 180, no. 15, 1965, pp. 371–376.

[32] M. Raghavan, "The Stewart platform of general geometry has 40 configurations," *Journal of Mechanical Design*, vol. 115, no. 2, pp. 277–282, Jun. 1993.

[33] M. L. Husty, "An algorithm for solving the direct kinematics of general Stewart-Gough platforms," *Mechanism and Machine Theory*, vol. 31, no. 4, pp. 365–379, May 1996.

[34] T.-Y. Lee and J.-K. Shim, "Improved dialytic elimination algorithm for the forward kinematics of the general Stewart-Gough platform," *Mechanism and Machine Theory*, vol. 38, no. 6, pp. 563–577, Jun. 2003.

[35] W. G. Breckenridge, "Quaternions – Proposed standard conventions," Jet Propulsion Laboratory, Pasadena, CA, Interoffice Memorandum IOM 343-79-1199, 1999.

[36] N. Trawny and S. I. Roumeliotis, "Indirect Kalman filter for 3D pose estimation," University of Minnesota, Dept. of Comp. Sci. & Eng., MARS Lab, Tech. Rep. 2005-002, Jan. 2005.
[37] B. K. P. Horn, "Closed-form solution of absolute orientation using orthonormal matrices," *Journal of the Optical Society of America. A, Optics and Image Science*, vol. 5, no. 7, pp. 1127–1135, Jul. 1988.
[38] ——, "Closed-form solution of absolute orientation using unit quaternions," *Journal of the Optical Society of America. A, Optics and Image Science*, vol. 4, no. 4, pp. 629–642, Apr. 1987.
[39] C. W. Wampler, "Forward displacement analysis of general six-in-parallel sps (Stewart) platform manipulators using soma coordinates," *Mechanism and Machine Theory*, vol. 31, no. 3, pp. 331–337, Apr. 1996.
[40] C. Innocenti, "Forward kinematics in polynomial form of the general Stewart platform," *Journal of Mechanical Design*, vol. 123, no. 2, pp. 254–260, Jun. 2001.
[41] J. Verschelde, "Algorithm 795: PHCpack: A general-purpose solver for polynomial systems by homotopy continuation," *ACM Trans. on Mathematical Software*, vol. 25, no. 2, pp. 251–276, Jun. 1999.
[42] I. A. Bonev and J. Ryu, "A new method for solving the direct kinematics of general 6-6 Stewart platforms using three extra sensors," *Mechanism and Machine Theory*, vol. 35, no. 3, pp. 423–436, Mar. 2000.
[43] D. Cox, J. Little, and D. O'Shea, *Ideals, Varieties, and Algorithms*, 3rd ed. New York, NY: Springer, 2008.
[44] A. Ansar and K. Daniilidis, "Linear pose estimation from points or lines," *IEEE Trans. on Pattern Analysis and Machine Intelligence*, vol. 25, no. 5, pp. 578–589, May 2003.
[45] L. Quan and Z.-D. Lan, "Linear n-point camera pose determination," *IEEE Trans. on Pattern Analysis and Machine Intelligence*, vol. 21, no. 8, pp. 774–780, Aug. 1999.
[46] W. Brogan, *Modern Control Theory*, 3rd ed. Upper Saddle River, NJ: Prentice Hall, 1991.
[47] P. S. Maybeck, *Stochastic Models, Estimation, and Control*. New York, NY: Academic Press, 1979, vol. 1.
[48] W. J. Rugh, *Linear System Theory*, 2nd ed. Upper Saddle River, NJ: Prentice Hall, 1996.
[49] R. Hermann and A. Krener, "Nonlinear controllability and observability," *IEEE Trans. on Automatic Control*, vol. 22, no. 5, pp. 728–740, Oct. 1977.
[50] X. S. Zhou, K. X. Zhou, N. Trawny, and S. I. Roumeliotis, "Interrobot relative pose controllability and observability," University of Minnesota, Dept. of Comp. Sci. & Eng., MARS Lab, Tech. Rep. 2007-001, Dec. 2007.
[51] S. M. Kay, *Fundamentals of Statistical Signal Processing: Estimation Theory*. Upper Saddle River, NJ: Prentice Hall, 1993.
[52] C.-C. Su, "Generalisation of radar doppler shift for target of arbitrary velocity relative to transceiver," *Electronics Letters*, vol. 36, no. 21, pp. 1812–1813, Oct. 2000.

Nikolas Trawny received the DEA in Control and Automation from ISAE (formerly SUPAERO) Toulouse, France in 2003, the Diploma of Aerospace Engineering from the University of Stuttgart, Germany, in 2004, and the M.Sc. in Computer Science from the University of Minnesota in 2008. He is currently a Ph.D. candidate at the Department of Computer Science and Engineering (CSE) at the University of Minnesota. His research interests lie in the areas of vision-aided inertial navigation and multi-robot localization and mapping. He is the recipient of the 2006 Guidant Award from the CSE Department of the University of Minnesota.

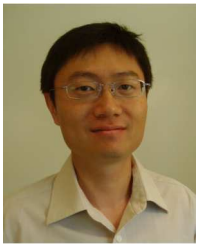

Xun S. Zhou received his B.Sc. in Physics with honors from the Zhongshan University, China in 2000, and the M.Sc. in Computer Science from the Bradley University, IL in 2003. He is currently a Ph.D. candidate in the Department of Computer Science and Engineering (CSE) at the University of Minnesota, MN. His research interests lie in the areas of single- and multi-robot systems, localization and mapping, and multi-sensor extrinsic calibration. He is the recipient of the 2007 Excellence in Research Award from the CSE Department of the University of Minnesota, and in 2006 he was the Finalist for the Best Paper Award of the IEEE/RSJ International Conference on Intelligent Robots and Systems.

Ke Zhou received his B.Sc and M.Sc in Control Science and Engineering from the Zhejiang University, China in 2001 and 2004 respectively. He is currently a Ph.D student in the Department of Electrical and Computer Engineering (ECE) at the University of Minnesota. His research interests lie in the areas of multi-robot systems, optimization and active sensing.

Stergios I. Roumeliotis received the Diploma in Electrical Engineering from the National Technical University of Athens, Greece, in 1995, and the M.S. and Ph.D. degrees in Electrical Engineering from the University of Southern California, CA in 1999 and 2000 respectively. From 2000 to 2002 he was a Postdoctoral Fellow at the California Institute of Technology, CA. Between 2002 and 2008 he was an Assistant Professor with the Department of Computer Science and Engineering, University of Minnesota, MN, where he is currently an Associate Professor. Since 2009, S.I. Roumeliotis is the Associate Director for Research of the Digital Technology Center (DTC). His research interests include vision-aided inertial navigation of aerial and ground autonomous vehicles, distributed estimation under communication and processing constraints, and active sensing for reconfigurable networks of mobile sensors.

S.I. Roumeliotis is the recipient of the Guillermo E. Borja Award (2009), the National Science Foundation (NSF) Presidential Early Career Award for Scientists and Engineers (PECASE) (2008), the NSF CAREER award (2006), the McKnight Land-Grant Professorship award (2006-08), the ICRA Best Reviewer Award (2006), and he is the co-recipient of the One NASA Peer award (2006), and the One NASA Center Best award (2006). Papers he has co-authored have received the Robotics Society of Japan Best Journal Paper award (2007), the ICASSP Best Student Paper award (2006), the NASA Tech Briefs award (2004), and three of them were Finalists for RSS Best Paper Award (2009), the ICRA Best Student Paper Award (2009) and the IROS Best Paper Award (2006). S.I. Roumeliotis is currently serving as Associate Editor for the IEEE Transactions on Robotics.